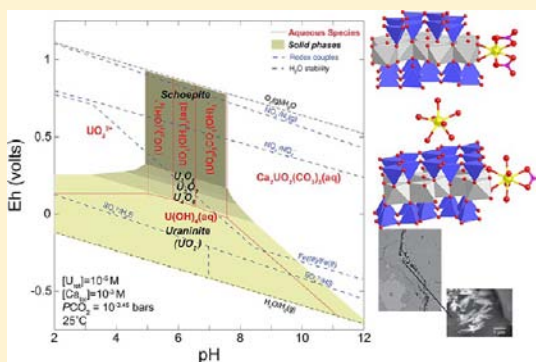


Environmental Speciation of Actinides

Kate Maher,^{*,†} John R. Bargar,[‡] and Gordon E. Brown, Jr.^{†,‡,§}[†]Department of Geological & Environmental Sciences, Stanford University, Stanford, California 94305-2115, United States[‡]Stanford Synchrotron Radiation Lightsource and [§]Department of Photon Science, SLAC National Accelerator Laboratory, 2575 Sand Hill Road, MS 69, Menlo Park, California 94025, United States

ABSTRACT: Although minor in abundance in Earth's crust (U, 2–4 ppm; Th, 10–15 ppm) and in seawater (U, 0.003 ppm; Th, 0.0007 ppm), light actinides (Th, Pa, U, Np, Pu, Am, and Cm) are important environmental contaminants associated with anthropogenic activities such as the mining and milling of uranium ores, generation of nuclear energy, and storage of legacy waste resulting from the manufacturing and testing of nuclear weapons. In this review, we discuss the abundance, production, and environmental sources of naturally occurring and some man-made light actinides. As is the case with other environmental contaminants, the solubility, transport properties, bioavailability, and toxicity of actinides are dependent on their speciation (composition, oxidation state, molecular-level structure, and nature of the phase in which the contaminant element or molecule occurs). We review the aqueous speciation of U, Np, and Pu as a function of pH and Eh, their interaction with common inorganic and organic ligands in natural waters, and some of the common U-containing minerals. We also discuss the interaction of U, Np, Pu, and Am solution complexes with common Earth materials, including minerals, colloids, gels, natural organic matter (NOM), and microbial organisms, based on simplified model system studies. These surface interactions can inhibit (e.g., sorption to mineral surfaces, formation of insoluble biominerals) or enhance (e.g., colloid-facilitated transport) the dispersal of light actinides in the biosphere and in some cases (e.g., interaction with dissimilatory metal-reducing bacteria, NOM, or Mn- and Fe-containing minerals) can modify the oxidation states and, consequently, the behavior of redox-sensitive light actinides (U, Np, and Pu). Finally, we review the speciation of U and Pu, their chemical transformations, and cleanup histories at several U.S. Department of Energy field sites that have been used to mill U ores, produce fissile materials for reactors and weapons, and store high-level nuclear waste from both civilian and defense operations, including Hanford, WA; Rifle, CO; Oak Ridge, TN; Fernald, OH; Fry Canyon, UT; and Rocky Flats, CO.



INTRODUCTION

Over the last century, the mining and processing of uranium ores and the manufacturing and testing of nuclear weapons have created a legacy of contamination of uranium and other actinides in soils and groundwater, particularly at U.S. Department of Energy (U.S. DOE) sites that have manufactured nuclear weapons or store high-level radioactive waste. In addition, driven by the demand for more electricity and the need for alternative energy sources that emit less CO₂ than fossil fuels, there has been a renewed interest in nuclear power and advanced nuclear fuel cycles over the past decade.^{1,2} The projected acceleration in the development of uranium and thorium resources worldwide suggests that actinides will continue to pose a threat to the environment and water resources long into the future, unless improved methods for extraction, processing, and storage are developed and deployed.^{3,4}

In the United States, the long history of uranium mining, processing, and disposal provides a platform for evaluating the effects of improper handling of actinide-bearing waste solutions and solids and the efficacy of remediation strategies, particularly for uranium. For example, the speciation, mobility, and

transport of uranium at several U.S. DOE sites (e.g., Hanford, WA; Oak Ridge, TN; and Rifle, CO) and of plutonium at the Rocky Flats Environmental Technology Site near Denver, CO, have been studied extensively. This work has led to an enhanced understanding of uranium and plutonium speciation and biogeochemical dynamics under different environmental conditions and to the elucidation of key scientific challenges, particularly in the selection and optimization of remediation strategies. Further insight into the environmental behavior of actinides is gained from studies of the oxidative weathering of uranium ore deposits, such as Nopal I, Mexico,^{5–10} which provide examples of long-term processes that may govern the evolution of storage repositories.⁷

This review discusses the speciation of some of the most common actinides (Th, U, Np, and Pu) in aqueous solutions and in solids common in the environment, as well as their interactions with mineral surfaces, organic matter, and

Special Issue: Inorganic Chemistry Related to Nuclear Energy

Received: July 31, 2012

Published: November 8, 2012

microorganisms. We build on the many simplified model system studies that have been carried out on these elements during the past several decades and rely heavily on recent comprehensive reviews of environmental actinide speciation, including those by Choppin and Jensen,¹¹ Runde and Neu,¹² Degueldre,¹³ and Reed et al.¹⁴ in *The Chemistry of the Actinide and Transactinide Elements* edited by Morss et al.¹⁵ Our emphasis here is on uranium because this actinide is the most common one at contaminated U.S. DOE sites, is second only to thorium in natural abundance in the Earth's crust,¹⁶ and is by far the most studied. We also provide brief summaries of uranium speciation and dynamics at several U.S. DOE sites (Hanford, WA; Oak Ridge, TN; Rifle, CO; Fernald, OH; and Fry Canyon, UT) and plutonium speciation at the Rocky Flats, CO, site. These polluted sites have attracted a great deal of scientific and public attention over the past several decades and provide physically, chemically, and hydrologically complex environments with a rich diversity of different actinide contaminant species.

■ ABUNDANCE, PRODUCTION, AND ENVIRONMENTAL SOURCES OF ACTINIDES

Actinides consist of a group of radioactive metallic elements with atomic numbers (*Z*) between 89 (actinium) and 103 (lawrencium) with sequentially filled 5*f* atomic subshells (Figure 1). The heavier actinides (*Z* = 97–103) have short

| | 89 | 90 | 91 | 92 | 93 | 94 | 95 | 96 | 97 | 103 |
|---|-----------------------|------------------------------------|--|--|--|--|--|--|--|---|
| | Ac | Th | Pa | U | Np | Pu | Am | Cm | Bk | Lr |
| Valence electrons: | 6d 7s ² | 6d ² 7s ² | 5f ² 6d 7s ² | 5f ³ 6d 7s ² | 5f ⁴ 6d 7s ² | 5f ⁶ 6d 7s ² | 5f ⁷ 6d 7s ² | 5f ⁷ 6d 7s ² | 5f ⁷ 6d 7s ² | 5f ¹⁴ 6d 7s ² |
| Oxidation States: (all conditions) | III | III, IV | III, IV, V | III, IV, V, VI | III, IV, V, VI, VII | III, IV, V, VI, VII | III, IV, V, VI, VII? |
| Oxic zone: (groundwater) | III | IV | V | VI | V | IV, V, VI | IV, V | III | III | III |
| Suboxic zone: (microbially active) | III | IV | IV | IV | IV | VI | IV | III | III | III |
| Anaerobic zone: (microbially active) | III | IV | IV | IV | III | IV | III | III | III | III |

■ naturally abundant ■ natural and anthropogenic
■ primarily anthropogenic ■ anthropogenic/short-lived
★ fissile isotope(s)

Figure 1. Overview of actinides and their sources, electron configurations, and common valence states under different conditions. Np, Pu, Am, and Cm are the most important products of the nuclear fuel cycle, and U, Pu, Np, and Am have fissile isotopes. The isotopes of ²³⁷Np (*t*_{1/2} = 2.14 million years) and ²³⁹Pu (*t*_{1/2} = 24100 years) are important in the environment because of their long half-lives. Also shown are the most likely actinide oxidation states in groundwater as a function of the microbial activity and the corresponding biogeochemical zone (after Reed et al.¹⁴): (–) unstable; (?) claimed but unsubstantiated; (bold/red) most prevalent.

half-lives, are produced in low quantities, and are thus not considered to pose substantial risks to the environment. The isotopes of ^{233,235}U, ²³⁷Np, and ^{241,243}Am and all of the Pu isotopes are fissile, which raises additional concerns regarding storage security.¹ Generally, actinides show more variability in their oxidation states relative to the lanthanide group elements (Figure 1), which can make their fate in the environment more challenging to study, and thus approaches for addressing these challenges will be a key focus of this review.

Thorium and uranium are the only naturally abundant actinides, with typical crustal concentrations of 10–15 and 2–4 ppm, respectively, although geochemical processes have concentrated uranium and thorium in particular environments to form economic deposits.¹⁶ The isotopes ²³²Th, ²³⁵U, and ²³⁸U are each progenitors of long α - and β -decay chains that result in the production of relatively short-lived ²³¹Pa, ^{230,234}Th, and ^{227,228}Ac daughter isotopes.¹⁷ In uranium-rich ore deposits, trace amounts of other actinide isotopes, primarily ²³⁷Np and ²³⁹Pu, can be produced naturally by neutron capture of ²³⁵U and ²³⁸U, respectively.¹⁸ Notable examples of neutron capture reactions occurring in nature are the natural fission reactors found at the Oklo and Bagombé uranium deposits in the Republic of Gabon. Approximately 2 billion years ago, when the natural ²³⁵U/²³⁸U ratio was 3.7% (a value much higher than the current value of 0.725%, but typical of light water reactors), sustained fission reactions occurred within these uranium-rich deposits.¹⁹ Over the course of the natural reactor lifespans (0.6–1.5 million years), ~2–3 tons of ²³⁹Pu and ~6 tons of fission products were produced.²⁰

The remaining actinides are only produced in high-energy neutron-rich environments typical of nucleosynthesis, nuclear reactors, and nuclear explosions. Models for nucleosynthesis based on the characteristic energy output of a supernova explosion, nuclear structure, decay energies, and half-lives require that ²⁵⁴Cm and other actinides were synthesized only via rapid neutron capture (e.g., the *r*-process) during core collapse supernovae.^{21–23} Because of the short half-lives associated with neutron-rich nuclei, the majority of the actinides underwent a series of α and β decays and spontaneous fission reactions to form lighter elements with *Z* < 92. The abundance of fission products and other daughter isotopes measured in meteorites (e.g., ¹³⁶Xe from fission of ²⁴⁴Pu) confirms that actinides were more abundant in the early solar system.²⁴

Today, aside from the naturally occurring actinides (primarily uranium and thorium and their daughters), the global inventory of actinides is derived from nuclear reactors and nuclear explosions.¹² As a result, the majority of actinides, in particular plutonium, neptunium, americium, and curium, are released to the environment from human activities. Although the beneficial and industrial applications for some actinides are growing, as targets or byproducts of the nuclear industry and in weapons production, the majority of actinides have been released to the environment at different stages of the nuclear fuel cycle, primarily through (1) improper disposal of mine tailings and effluents, (2) direct discharges from enrichment and processing plants to the atmosphere, (3) disposal of high-level waste and highly contaminated solvents into groundwater and surface waters either directly or as a result of faulty storage containment, (4) dispersion from atmospheric and below-ground nuclear weapons testing, and (5) accidental releases from reactors. For a full summary of global inventories and releases as a consequence of the above activities, see Runde and Nue.¹² A final important consideration in evaluating the environmental consequences of actinide releases is their activities (e.g., the product of the decay constant and the number of atoms) and their half-lives. For example, even though uranium is generally abundant at contaminated sites on a mass-per-volume basis, the short-lived isotopes of americium and plutonium, even at substantially lower concentrations, can pose a much greater health risk because of their much higher activities.²⁵

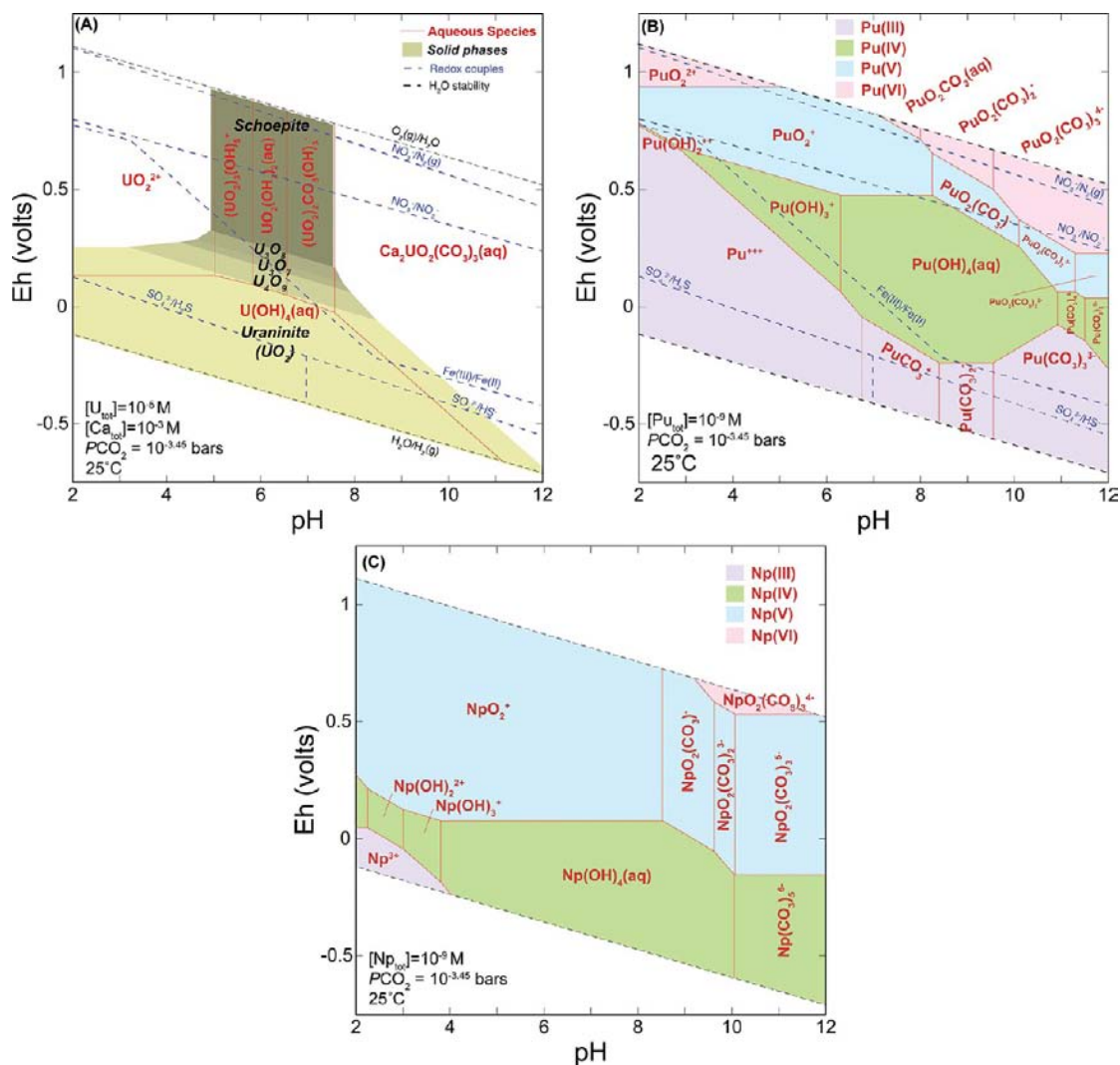
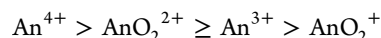


Figure 2. Pourbaix diagrams for uranium, plutonium, and neptunium in the environment. (A) Predominance domains of the major aqueous species and minerals shown as a function of the Eh (V) and pH for total uranium $[U_{\text{Tot}}] = 10^{-5}$ M in water containing calcium ions ($[Ca_{\text{Tot}}] = 10^{-3}$ M) and in equilibrium with atmospheric CO_2 ($P_{\text{CO}_2} = 10^{-3.45}$ bars). Dashed lines define the environmentally relevant redox couples are also shown for reference. (B) Plutonium speciation where colors represent the different oxidation states and the corresponding aqueous speciation (see the text for a discussion of likely minerals). (C) Neptunium speciation with oxidation states represented in colors as in part B. Diagrams are calculated using the Geochemist's Workbench and the LLNL V8 R6 "combined" database. Uranium aqueous species are from Guillaumont et al.³¹ and Dong and Brooks.³²

■ AQUEOUS SPECIATION OF URANIUM AND OTHER ACTINIDES

The primary factor determining the mobility of actinides (An) in the environment is their oxidation state, which can have a wide range of values depending on environmental redox conditions, as shown in Figure 1. Thorium, americium, and curium exist in only one oxidation state (Th^{4+} , Am^{3+} , and Cm^{3+}) over the range of common groundwater redox conditions. Uranium, neptunium, and plutonium are multivalent under subsurface conditions and exist as An^{3+} , An^{4+} , AnO_2^+ , or AnO_2^{2+} species. Reduction of higher-valent actinides to An^{3+} and An^{4+} species results in lower solubility and a heightened tendency to sorb on mineral surfaces. In these lower oxidation states, actinides form hydrated An^{3+} and An^{4+} ions, whereas in the V and VI oxidation states, they are unstable in aqueous solution and hydrolyze instantly to form linear *trans*-dioxo(actinyl) cations, AnO_2^+ and AnO_2^{2+} , respectively.^{26–28}

The strength of the actinide complexes (for a particular ligand) generally decreases in the order



with tetravalent actinides forming stable aqueous complexes and solid phases with low solubility and pentavalent actinides forming the least stable complexes and more soluble solid phases.¹¹ Given the generally high solubilities and hence mobilities of the actinides in a higher oxidation state, these are of primary concern in an environmental context.

Microbes, when present in subsurface environments, can play a major role in defining the predominant oxidation state of the actinide through enzymatic pathways.¹⁴ Multivalent actinides can be reduced to their lowest oxidation states by microbial processes in suboxic and anaerobic biogeochemical zones (Figure 1). Abiotic reduction of actinides is also possible when the oxidized species accept electrons from Fe^{2+} -containing minerals, as is oxidation when reduced species transfer

electrons to Fe^{3+} -containing minerals, which are among the most abundant and important natural inorganic sorbents. Radiolysis of actinides in solution can also produce highly reactive species such as e^-_{aq} , H^\bullet , OH^\bullet , and H_2O_2 , which can induce changes in the solute, including the actinide oxidation state.^{29,30}

For uranium, oxidized hexavalent uranium is highly soluble as the uranyl ion UO_2^{2+} , whereas the solubility of U^{IV} is largely controlled by insoluble oxides such as uraninite (UO_2 ; Figure 2). Under oxidizing conditions typical of surface waters and some groundwater systems, the aqueous speciation of U^{VI} may determine the partitioning of uranium onto mineral surfaces, the reduction of U^{VI} to U^{IV} , and the mode of incorporation of uranium into secondary precipitates such as iron (oxyhydr)-oxides. Hydrolysis of the uranyl ion becomes important above $\text{pH} \sim 4$, where hydroxo complexes compete with other inorganic and organic ligands in solution, including carbonate, phosphate, sulfate, silicate, and *n*-carboxylic and humic acids (Figures 2 and 3).^{31–34} For example, in the presence of

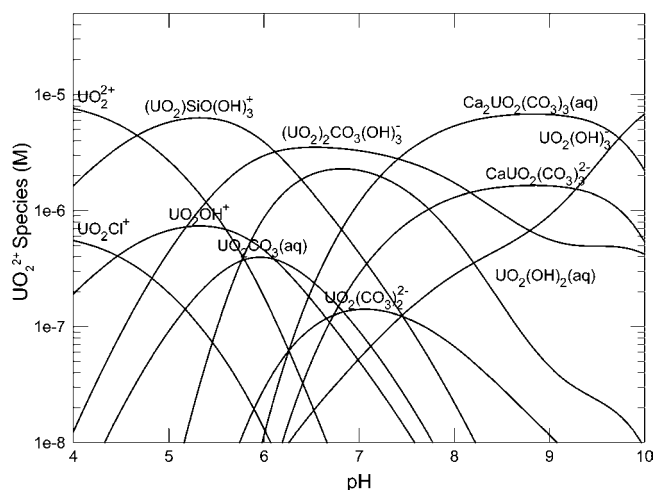
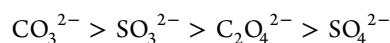


Figure 3. Distribution of solution-phase U^{VI} species in the presence of water, carbonate, calcium, and $\text{SiO}_2(\text{aq})$: $[\text{U}^{\text{VI}}_{\text{T}}] = 10^{-5}$ M in the presence of water, $[\text{Ca}_{\text{Tot}}] = 10^{-2}$ M, $[\text{SiO}_2(\text{aq})] = 10^{-2.5}$ M, and atmospheric CO_2 ($P_{\text{CO}_2} = 10^{-2.5}$ bars).

carbonate and other cations, the uranyl ion forms a series of neutral, anionic binary, and polynuclear species that can influence adsorption of uranium on mineral surfaces^{35–38} and inhibit both the abiotic and biotic reduction of uranium.^{39–43} In general, the binary species are the most stable aqueous species, but polynuclear species, particularly in the neutral to alkaline pH range, can be important for uranium mobility. Aqueous complexation of uranium (and the other actinides) has been studied using a variety of techniques, including calorimetric or potentiometric titration,^{44–48} time-resolved laser-induced fluorescence spectroscopy,^{49–51} Raman spectroscopy,⁵² attenuated total-reflectance Fourier transform infrared spectroscopy,^{52,53} and extended X-ray adsorption fine-structure (EXAFS) spectroscopy,^{53–57} and through application of ab initio quantum chemical approaches such as density functional theory.^{56,58} The most recent evaluation of thermodynamic data regarding the aqueous speciation of uranium is described in Guillaumont et al.,³¹ although data for some species, particularly organic ligands, were not reviewed for this compilation. Berto et al.³³ also provide a thorough review of the aqueous coordination chemistry of uranyl, along with a compilation of stability

constants, including the major organic and inorganic ligands. In general, the tendency of actinide ions to form complexes with univalent or bivalent inorganic ligands follows the trends¹¹



Because of their ubiquity in natural waters, hydroxide and carbonate are the most important ligands for actinide complexation.

Chelation of UO_2^{2+} by organic compounds may be as important as inorganic complexation in many natural systems and at contaminated sites where organic chelators were used in actinide processing. Organic ligands, from simple carboxylic acids to more complex humic acids, are present at variable concentrations in most natural waters.⁵⁹ For example, in oil-field brines, acetic acid concentrations can approach thousands of parts per million,⁶⁰ whereas surface and shallow groundwaters typically contain di- and tricarboxylic acids at concentrations of ~ 10 – 100 ppm⁶¹ and a high proportion of humic acids.^{59,62} Uranium forms stable complexes with a variety of organic ligands, and organic-chelated uranyl species can be highly mobile.^{33,44–48,52,54,55,63–65} Pompe et al.⁶⁶ found that natural and synthetic humic acids complex U^{VI} and may also play a role in Pu^{VI} complexation. Thorium(IV) humate complexes have also been reported.⁶⁷ When the organic chelate has the proper steric arrangement to form small chelate rings with the equatorial oxygen atoms on the uranyl ion (e.g., the carboxylate groups in oxalate or citrate), the uranyl chelates can have exceptionally high stability.⁴⁴ As a result, the industrial use of chelating agents, such as Tiron or citrate, to enhance the mobility of uranyl is common in industrial applications, and organic chelation of uranyl has been used to remove uranium from contaminated soils during pump-and-treat remediation strategies.⁶⁸ The mobilization and transport of uranium by carboxylic acids and organic compounds is also thought to be important in the formation of sedimentary uranium ore deposits.^{69,70} At low pHs, where uranyl adsorption onto mineral surfaces is not favored by charge considerations, functional groups associated with natural organic matter (NOM) adsorbed to mineral surfaces may enhance UO_2^{2+} sorption.^{71,72} Alternatively, binding of uranyl to the cell envelope of microbial organisms may inhibit cell metabolism⁷³ or inhibit uranium reduction, with consequences for the effectiveness of bioremediation strategies. In addition, plutonium and americium have been found to associate preferentially with dissolved high-molecular-weight organic matter.⁷⁴ NOM can also cause reduction of redox-sensitive actinides, including neptunium and plutonium.^{75–77} Interactions between natural and amended synthetic organic compounds can thus play a key role in determining the fate of actinides in the environment.

Aqueous speciation of plutonium and neptunium is also shown in Figure 2B,C (solid phases are not shown in the diagram because of considerable uncertainty surrounding the solubility and identity of the dominant secondary phases).^{78,79} The dominance of the carbonate complexes under natural conditions at near-neutral and basic pHs is a common feature of all three actinides. However, there are some key differences among uranium, plutonium, and neptunium speciation. Plutonium has the most complex redox chemistry of the actinides, with multiple valence states stable under typical pH and redox conditions of subsurface environments. Plutonium speciation is thus a strong function of the Eh, pH, ionic

strength, organic and inorganic ligands, and disproportionation kinetics. Because the redox couples of $\text{Pu}^{\text{III}}/\text{Pu}^{\text{IV}}$ and $\text{Pu}^{\text{V}}\text{O}_2^+/\text{Pu}^{\text{VI}}\text{O}_2^{2+}$ are less negative than the $\text{Pu}^{\text{IV}}/\text{Pu}^{\text{VI}}\text{O}_2^+$ couple, multiple oxidation states can be present in solution as a result of plutonium disproportionation, which becomes increasingly favorable at elevated temperature and at $\text{pH} < 1.5$ and > 7 .¹¹ Although Pu^{V} and Pu^{VI} predominate under oxic conditions, in general, Pu^{IV} is often the most common plutonium ion at neutral pH and mildly reducing conditions, whereas Pu^{III} tends to have much lower solubility. Pentavalent plutonium can be reduced to Pu^{IV} via adsorption on mineral surfaces (including redox-inactive minerals), although the exact mechanism and kinetics are not well established.^{80–83} In the tetravalent state, the aggregation of hydrolysis products (e.g., $[\text{Pu}(\text{OH})_n]^{(4-n)+}$) results in the formation of hydroxo-bridged polymers.⁸⁴ The formation of stable colloids of polymeric plutonium(IV) hydroxide is known to greatly enhance the mobility of Pu^{IV} in the environment, as discussed in later sections. At the concentrations shown in Figure 2B (10^{-9} M Pu_{tot}), $\text{Pu}(\text{OH})_4(\text{s})$ is found to control the Pu^{IV} solubility.¹² If crystalline $\text{PuO}_2(\text{s})$ is considered the dominant control on plutonium solubility, the concentration of Pu^{IV} would be $\sim 10^{-17}$ M. PuO_2^+ does not tend to form strong complexes with inorganic anions within the low-to-neutral pH range, whereas PuO_2^{2+} forms complexes with Cl^- and NO_3^- anions, which are comparatively less stable than Pu^{IV} complexes. However, Pu^{III} , Pu^{IV} , and Pu^{VI} will form mono- to polymolecular complexes with many organic ligands such as acetate, oxalate, and ethylenediaminetetraacetic acid.⁸⁵ Such complexes would limit the polymerization of plutonium(IV) hydroxides and are thus often used in plutonium separations.

In contrast to uranium and plutonium, pentavalent neptunium is stable under oxic to moderately suboxic conditions as the *trans*-dioxoneptunyl cation NpO_2^+ or as neptunylcarbonato complexes at high pH (Figure 2B).¹³ As a result, neptunium is generally the most soluble and mobile of the actinides and perhaps the greatest concern to waste storage sites. Np^{IV} is favored in anoxic environments and hydrolyzes to form polymeric hydroxides, similar to Pu^{IV} . Tetravalent neptunium is commonly incorporated into sparingly soluble solids such as $\text{Np}(\text{OH})_4$ or immobilized via the formation of strong surface complexes with aquifer solids. Depending on the redox conditions, neptunium solubilities are also likely to be limited to $\sim 10^{-8}$ to $\sim 10^{-4}$ M by poorly crystalline oxyhydroxides $[\text{Np}^{\text{IV}}(\text{OH})_4(\text{s})]$ or oxides $[\text{Np}^{\text{V}}\text{O}_5(\text{s})]$, respectively.^{12,78} Although NpO_2 is thermodynamically favored, it has not been identified in solubility experiments involving natural waters—only amorphous Np^{IV} solid phases precipitated, and hence these are thought to control aqueous neptunium concentrations, at least initially.^{78,86}

The aqueous speciation of actinides serves as the foundation for assessing actinide mobility in the environment because the oxidation state and predominance of aqueous complexes determine their interactions with mineral and microbial surfaces, as well as the formation of solid phases, from colloids to bulk amorphous and crystalline precipitates. The aqueous speciation of actinides is thus a critical area for continued study, especially as mineralogical sequestration and in situ bioremediation efforts using direct or enzymatic reduction of uranium continue to be explored.

■ REACTIONS OF ACTINIDE SPECIES WITH MINERAL SURFACES, GELS, ORGANICS, AND MICROORGANISMS

Sorption of Actinides on Mineral Surfaces. Ultimately, the mobility of actinides in near- and far-field environments is known to be a strong function of the competition between aqueous and mineral surface complexation reactions and sorption reactions.^{87,88} The term *sorption* as used here implies the partitioning of a solution complex to a solid, NOM fixed in the aquifer matrix, or nonplanktonic microbial organisms in contact with the solution.^{89,90} Sorption may involve relatively weak electrostatic interaction or hydrogen bonding of a solution complex with a solid surface without loss of any waters of hydration from the complex. This type of interaction results in an *outer-sphere surface complex*. Sorption may also involve direct covalent interaction of the solution complex with the solid surface in which one or more waters of hydration are lost and the sorbing atom forms one or more covalent bonds to one or more types of reactive sites on the solid surface, which are typically hydroxo or oxo groups, depending on the solution pH, on most mineral surfaces in contact with oxic water. This stronger type of interaction results in an *inner-sphere surface complex*. Inner-sphere complexes can be mononuclear or multinuclear, depending on the surface loading and other factors. In addition, both inner- and outer-sphere complexes involving the same sorbate species can occur on a solid surface simultaneously (e.g., Catalano et al.⁹¹). Sorbate species may also be incorporated into three-dimensional *solid precipitates*, which may result from nucleation and growth of a solid made up of sorbate ions on a sorbent particle surface or from release of ions from the sorbent particle through dissolution reactions followed by coprecipitation of these ions with sorbate ions in solution to form a three-dimensional solid (e.g., Towle et al.⁹²). Inner-sphere surface complexes reduce the mobility of sorbates to a greater extent than more weakly bound outer-sphere surface complexes, although even inner-sphere surface complexes may be desorbed if the solution pH or dissolved actinide concentrations are diminished or the ionic strength increases over time. Moreover, the incorporation of a sorbate ion into a solid precipitate can result in even stronger sequestration of the sorbate species, particularly if the precipitate has a low solubility product. Molecular-level knowledge of the types of sorbed species and their behavior under different conditions is critical for predicting their mobility and fate in the environment, and molecular-level measurements of sorbate speciation are now becoming relatively routine, even for complex environmental samples.^{93,94}

Sorption of actinides onto mineral surfaces, NOM, and microbial organisms, including microbial biofilms, depends in part on their speciation, particularly their oxidation state. For example, the following order of actinide sorption is generally observed in laboratory studies: $\text{An}^{4+} > \text{An}^{3+} > \text{AnO}_2^{2+} \gg \text{AnO}_2^+$. In addition, different mineral surfaces show significant differences in reactivity with respect to a common adsorbing ion. A good example of this comes from a macroscopic uptake study of Np^{V} on various mineral surfaces with different pH_{PZC} values (pH values where the net surface charge is zero) by Kohler et al.⁹⁵ (Figure 4), who found the following order of affinities of the different sorbents for Np^{V} [with the compositions and approximate pH_{ads} values (the pH at 50% of the maximum Np^{V} uptake) given in parentheses and the adsorption edge data normalized to equimolar surface sites]:

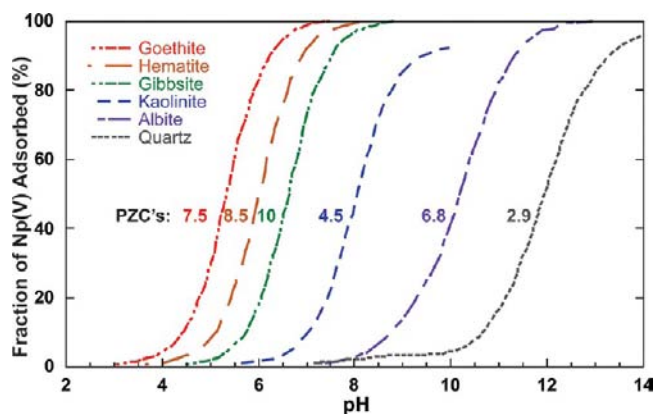


Figure 4. Adsorption isotherms of aqueous Np^{V} on various mineral surfaces as a function of the pH in the absence of competing ligands. The pH_{PZC} of each mineral is given in the plot. All of the uptake data were normalized to 5×10^{-4} equimolar surface sites and the Np^{V} concentration was $(1.1\text{--}1.3) \times 10^{-7}$ M at 0.1 M NaCl background electrolyte concentration (after Kohler et al.⁹⁵).

goethite ($\alpha\text{-FeOOH}$: 5.5) > hematite ($\alpha\text{-Fe}_2\text{O}_3$: 6.0) > gibbsite ($\alpha\text{-Al(OH)}_3$: 6.8) > kaolinite ($\text{Al}_2\text{Si}_2\text{O}_5(\text{OH})_4$: 8.2) > albite ($\text{NaAlSi}_3\text{O}_8$: 10.3) > quartz ($\alpha\text{-SiO}_2$: 12).

Np^{V} in the form of neptunyl species (NpO_2^+) sorbs essentially completely on the goethite, hematite, and gibbsite surfaces at pH values below their respective pH_{PZC} values, where the mineral surface is positively charged. The pH_{PZC} values of these sorbents are given in Figure 4 (values from Sverjensky,⁹⁶ except for goethite⁹⁷ and kaolinite^{98,99}). Thus, NpO_2^+ forms relatively strong chemical bonds with surface functional groups on goethite, hematite, and gibbsite as found for Np^{V} on goethite by EXAFS spectroscopy.¹⁰⁰ In contrast, sorption of NpO_2^+ on the other phases occurs well above their pH_{PZC} values, suggesting that the bonds between NpO_2^+ and surface functional groups on these sorbents are not as strong or that the adsorption free energy must include a repulsive term.¹⁰¹ This example shows that quartz, in particular, is a poor sorbent of NpO_2^+ , as well as of other actinides.

Although quartz is not an effective sorbent for actinides, other common minerals are, including iron (oxyhydr)oxides such as goethite, hematite, magnetite, and ferrihydrite, manganese (oxyhydr)oxides such as birnessite, hausmannite, and manganite, clay minerals such as montmorillonite, kaolinite, and bentonite, zeolites such as clinoptilolite, carbonates such as calcite, and phosphates such as apatite. All of these minerals are relatively abundant in various geological settings where actinide contaminants are present, and they are often in high-surface-area forms, either as nanoparticles/colloids or as coatings on the surfaces of other minerals, and thus are the dominant solid phases to which actinide species sorb. An excellent example of the preferential association of actinides with certain mineral phases comes from a $\mu\text{-XANES}$ (X-ray absorption near-edge structure) spectroscopy and synchrotron-based $\mu\text{-XRF}$ (X-ray fluorescence) elemental imaging study by Duff et al.¹⁰² In laboratory sorption experiments, they found that plutonium associates with manganese (oxyhydr)oxide coatings and with smectites in Yucca Mountain Tuff but not with iron (oxyhydr)oxides, whose surfaces were thought to have been passivated. In addition, this study showed that Pu^{V} is oxidized to Pu^{VI} on these coatings. As pointed out in our discussion of the Fry Canyon, UT, field site later in this review, the more effective mineral sorbents can also be used in permeable

reactive barriers designed to remove contaminant species like U^{VI} from groundwater.

Macroscopic uptake studies of actinide species onto mineral surfaces, such as the Np^{V} study discussed above, are extremely useful for understanding their sorption behavior. However, such studies cannot provide molecular-level details about the structures and compositions of actinide complexes bound to solid surfaces. Spectroscopic or X-ray scattering studies must be carried out to derive such information. An example of a molecular-level study of the interaction of U^{VI} with mineral surfaces is the sorption of UO_2^{2+} on Wyoming montmorillonite (SWy-2), which Catalano and Brown³⁸ studied using EXAFS spectroscopy. At low pH (~ 4) and low ionic strength (10^{-3} M), uranyl has an EXAFS spectrum indistinguishable from the aqueous uranyl cation, indicating uranyl is fully solvated and binds via cation exchange in the interlayer position (Figure 5).

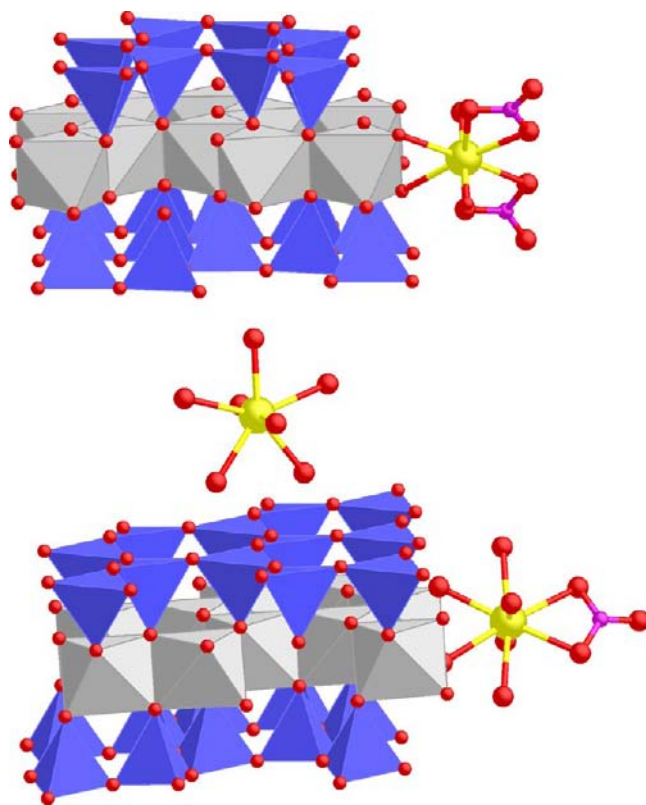


Figure 5. Uranyl and uranylcarbonato sorption complexes at montmorillonite/water interfaces and in interlayer regions revealed by U L_{III} -edge XAFS spectroscopy (after Catalano and Brown³⁸). Yellow balls are uranium, and red balls are oxygen. Montmorillonite is represented as polyhedra of SiO_4 tetrahedra (blue) and AlO_6 and FeO_6 octahedra (gray). Figure courtesy of J. G. Catalano.

At near-neutral pH (~ 7) and high ionic strength (1 M), the equatorial oxygen shell of uranyl is split, indicating inner-sphere binding to edge sites (Figure 5). This study concluded that cation exchange at low ionic strengths on SWy-2 may be more important than predicted by past surface complexation models of UO_2^{2+} adsorption on related montmorillonites. Analysis of the binding site on the edges of montmorillonite suggests that UO_2^{2+} sorbs preferentially to $[\text{Fe}(\text{O},\text{OH})_6]$ octahedral sites over $[\text{Al}(\text{O},\text{OH})_6]$ sites. When bound to edge sites, UO_2^{2+} occurs as uranylcarbonato ternary surface complexes. Polymeric surface complexes were not observed under any of the

conditions studied. Current surface complexation models of uranyl sorption on clay minerals should be reevaluated to account for the possible increased importance of cation-exchange reactions at low ionic strengths, the presence of reactive octahedral iron surface sites, and the formation of uranylcarbonato ternary surface complexes. Considering the adsorption mechanisms observed in the study by Catalano and Brown,³⁸ future studies of U^{VI} transport in the environment should consider how uranium retardation will be affected by changes in key solution parameters, such as the pH, ionic strength, exchangeable cation composition, and presence or absence of CO_2 . The findings of this study are consistent with the generalization that actinides may be adsorbed via an ion-exchange mechanism under acidic solution conditions where uptake of positively charged actinide species is generally low. However, as the pH increases to the near-neutral range and hydrolysis of actinide solution complexes is more favored, uptake is maximized. At higher pH values, actinide uptake is generally reduced because of the formation of anionic hydroxo or carbonato actinide complexes in solution.

The carbonate oxoanion is an important component of soil and aquatic systems and forms strong complexes with actinyl ions such as UO_2^{2+} at circum-neutral and higher pH (Figure 3). Consequently, as shown in Figure 6, at pH values >8, uranyl

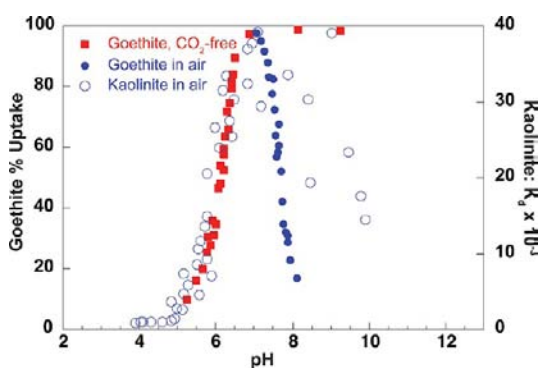


Figure 6. (A) Effect of the pH and CO_2 on the sorption of UO_2^{2+} on goethite and kaolinite^{103,104} (after Thompson et al.¹⁰⁵).

adsorption complexes on goethite and kaolinite surfaces can be desorbed in favor of the formation of this solution complex.^{36,103–105} In an earlier EXAFS study, Chisholm-Brause et al.¹⁰⁶ also found that uranyl binds to several different sites on montmorillonite. More recently, Bargar et al.^{35,107} showed that stable uranium(VI) carbonato complexes can form on hematite surfaces. Subsequent studies have shown that Ca^{2+} can competitively inhibit the adsorption of uranylcarbonato complexes on quartz and ferrihydrite surfaces because of the formation of stable $CaUO_2(CO_3)_3^{2-}$ and $Ca_2UO_2(CO_3)_3^0$ aqueous complexes.^{108,109}

There have been many EXAFS spectroscopic studies of the compositions, geometries, and binding modes of U^{VI} sorption complexes at mineral/water interfaces over the past 20 years (see Brown and Sturchio,¹¹⁰ Geckeis and Rabung,⁸⁸ Antonio and Soderholm,¹¹¹ and Tan et al.¹¹² for reviews of some of these studies). More recent studies include U^{VI} /montmorillonite,^{113–115} U^{VI} /kaolinite,¹¹⁶ U^{VI} /feldspar,¹¹⁷ U^{VI} /ferric oxides,^{118–120} $U^{VI}/\gamma-Al_2O_3$,^{121,122} U^{VI} /calcite,^{123,124} and U^{VI}/MnO_2 .¹²⁵ These studies have generally shown that U^{VI} forms dominantly inner-sphere complexes on oxygen-based mineral surfaces, typically with bidentate linkages to surface oxo groups.

Th^{IV} , Np^{V} , and Am^{III} have also been found to form inner-sphere complexes on various mineral surfaces using EXAFS and X-ray photoelectron spectroscopies.^{80,115,117,126–131}

Interaction of U^{6+} with Iron (Oxyhydr)oxides. In addition to forming sorption complexes on iron (oxyhydr)oxide surfaces, actinide ions such as UO_2^{2+} can also be sequestered through the incorporation into or physical association with iron (oxyhydr)oxides such as ferrihydrite and their transformation products.^{132,133} However, this alternative sequestration mechanism is not fully understood. For example, we do not know how the incorporation of common impurities associated with natural ferrihydrites, such as Al^{3+} or Si^{4+} , impact (promote or retard) the additional incorporation of trace impurities such as UO_2^{2+} . A prerequisite to achieving this understanding is detailed knowledge of natural nanominerals such as ferrihydrite, which is poorly crystalline and typically shows two diffuse diffraction lines for the common ferrihydrite nanoparticle size range (1–2 nm). In a baseline study of the ferrihydrite structure, a high-energy (90 keV) total X-ray scattering experiment on synthetic two-line ferrihydrite was carried out as a function of aging in the presence of a citrate solution at 175 °C.¹³⁴ While aging under these conditions results in the formation of hematite in ~14 h, analysis of the atomic pair distribution functions and complementary physiochemical and magnetic data indicate the formation of intermediate ferrihydrite phases at aging times of ≤ 8 h with larger particle size (up to 12 nm), fewer defects (i.e., iron vacancies), less structural water, less lattice strain, and electron-spin ordering, which results in pronounced ferrimagnetism relative to its disordered antiferromagnetic ferrihydrite precursor. This study also showed that the two-line ferrihydrite structure determined by Michel et al.,¹³⁵ although highly defective, is topologically very similar to the ordered ferrimagnetic ferrihydrite structure and thus provides a basis for understanding structural constraints on the incorporation of impurity ions into the two-line ferrihydrite structure. The proposed structure of two-line ferrihydrite is shown in Figure 7 (together with a photograph of natural ferrihydrite) and consists of layers of edge-shared FeO_6 octahedra (Fe1 sites) in the xy plane

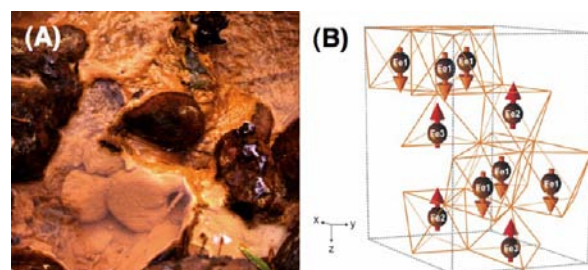


Figure 7. (A) Photograph of massive ferrihydrite in a stream bed in an acid mine drainage system associated with a mercury mine in central California. (B) Average hexagonal unit cell structure of ordered ferrimagnetic ferrihydrite (after aging for 8 h in the presence of a citrate solution at 175 °C) determined from high-energy total X-ray scattering and pair distribution analysis. Refinement of iron site occupancies in two-line ferrihydrite indicates that all of the Fe1 sites are occupied but only 50–55% of the Fe2 and Fe3 sites are occupied by Fe^{3+} , potentially allowing the precursor for $U^{6+/5+}$ incorporation. The arrows represent magnetic moments. The composition of disordered two-line ferrihydrite is $Fe_{8.2}O_{8.5}(OH)_{7.2} \cdot 3H_2O$, whereas the composition of ordered ferrimagnetic ferrihydrite (after aging) is $Fe_{10}O_{14}(OH)_2 \cdot 0.5–1.2H_2O$ (from Michel et al.¹³⁴).

connected along z by FeO_6 octahedra (Fe2 sites), which share edges with the Fe1 sites, and by FeO_4 tetrahedra (Fe3 sites), which share corners with Fe1 and Fe2 octahedra.¹³⁴ Refinement of the iron occupancies of these sites in two-line ferrihydrite showed that the Fe1 sites are completely filled by Fe^{3+} and that the Fe2 and Fe3 sites have 45–50% vacancies, which we suggest are occupied by three H^+ ions each to maintain a local charge balance.¹³⁴

A key issue in understanding how impurity ions (e.g., Al^{3+} , Si^{4+} , and U^{6+}) are incorporated in the ferrihydrite structure versus their physical association with ferrihydrite in separate phases is the effect of size differences of the substituting ions relative to $^{\text{VI}}\text{Fe}^{3+}$ and $^{\text{IV}}\text{Fe}^{3+}$. A general rule of thumb in the crystal chemistry of oxide and silicate minerals is that ions of the same charge can substitute for each other completely if their ionic radii differ by $\sim 10\%$ or less. The $\sim 17\%$ difference in the sizes of $^{\text{VI}}\text{Fe}^{3+}$ (0.645 Å) and $^{\text{VI}}\text{Al}^{3+}$ (0.535 Å) leads to the prediction of a partial solid solution of Al^{3+} in ferrihydrite, which is consistent with the extent of a solid solution of Al^{3+} in ferrihydrites reported in Cornell and Schwertman¹³⁶ (all ionic radius values are from Shannon¹³⁷). Similarly, the 20% difference in the sizes of $^{\text{IV}}\text{Fe}^{3+}$ (0.49 Å) and $^{\text{IV}}\text{Al}^{3+}$ (0.39 Å) suggests only a partial solid solution of Al^{3+} in the tetrahedral sites of ferrihydrite. In contrast, substitution of $^{\text{IV}}\text{Si}^{4+}$ (0.26 Å) for $^{\text{IV}}\text{Fe}^{3+}$ (0.49 Å) should be more limited because of the 47% difference in sizes and the limited number of tetrahedral sites in the average ferrihydrite structure ($\sim 20\%$ of the total iron sites). Moreover, it is highly unlikely that Si^{4+} can substitute for $^{\text{VI}}\text{Fe}^{3+}$ because Si^{4+} is very rarely found in octahedral coordination in minerals except in very high-pressure phases. Another consideration is the strain induced by substitutions of ions smaller (or larger) than Fe^{3+} in octahedral sites because of the shared edges between the octahedra in the average ferrihydrite structure, although this factor is more difficult to evaluate than simple size differences (e.g., ref 138). $^{\text{VI}}\text{U}^{6+}$ (0.73 Å) and $^{\text{IV}}\text{U}^{6+}$ (0.52 Å) are similar in size to $^{\text{VI}}\text{Fe}^{3+}$ and $^{\text{IV}}\text{Fe}^{3+}$, respectively, and on the basis of size differences alone, U^{6+} should substitute readily for Fe^{3+} in both the octahedral and tetrahedral sites of ferrihydrite. However, a serious issue with the substitution of U^{6+} for Fe^{3+} (or three H^+) in disordered ferrihydrite is the charge imbalance created locally. One way to compensate for potential overbonding of oxygen when $^{\text{VI}}\text{U}^{6+}$ substitutes for $^{\text{VI}}\text{Fe}^{3+}$ in an Fe1 site is to remove Fe^{3+} (or three H^+) from an adjacent Fe1 site, thus creating a coupled vacancy. Other substitution/vacancy combinations are also possible. Such a scenario would result in a local charge balance and satisfaction of Pauling's electrostatic valence principle. This type of reasoning allows crystal chemical constraints on impurity ion substitutions in ferrihydrites. It also provides some insight about the effect of impurity ions on the transformation of ferrihydrite into other iron (oxyhydr)oxides, because similar crystal chemical constraints will apply, and leads to testable hypotheses concerning the extent of impurity substitutions and phase transformations.

Interaction of U^{6+} with Gels. Another means of trapping uranium and other actinide species is illustrated by the study of Allard et al.,¹⁰ who were the first to determine the trapping mechanisms of uranium by gels during the oxidation of solutions percolating at a uranium mine site in the Massif Central in France. These gels result from the weathering of a uranium-mineralized granite in an acid-mine drainage system and, besides uranium, contain silicon, aluminum, and iron as major components (referred to as U-bearing Si-, Al-, and Fe-

rich gels). Al and Fe K-edge XANES and EXAFS showed that the local structures of these gels are similar to those of allophanes¹³⁹ and ferrihydrite.^{140,141} U L-edge XANES and EXAFS spectra showed that uranium is present as uranyl (UO_2^{2+}), with four equatorial oxygen neighbors. In the Si- and Al-rich gels, U–U pairs at 3.82 Å are consistent with edge-sharing uranyl, and U–Si pair correlations are consistent with the local structure of uranophane-group minerals. A coprecipitation process was suggested that involved silicon and uranium and resulted in the formation of proto-uranophane. The incorporation of actinides in Si- and Al-rich gels may also be a useful strategy for their sequestration at field sites when other sequestration approaches are not effective.¹⁴² This type of trapping mechanism of Cu^{II} ions in supergene weathering zones of porphyry copper deposits is responsible for formation of the common hydrated $\text{Cu}(\text{OH})_2$ -am- SiO_2 mixture known as chrysocolla.¹⁴³

Interaction of Actinides with NOM. The interaction of actinides with natural organic colloids is discussed in a later section of this paper and is reviewed by Runde and Neu¹² and by Choppin and Wong.¹⁴⁴ NOM consists of large-molecular-weight polyelectrolytes that have ill-defined and variable macromolecular structures depending on the pH and solution ionic strength.¹⁴⁵ ^{13}C NMR studies have revealed a number of different types of functional groups in NOM, many of which, particularly carboxylate, phenolate, and amino, can bind actinide species.^{146,147} A common approach to understanding the interaction of actinides and other metal ions with complex NOM is to study how they bind to simplified analogues of NOM such as acetate⁵⁵ and citrate,⁵⁴ although there have been some molecular-level spectroscopic studies of the interaction of actinides with NOM, including An^{III} interactions with humate¹⁴⁸ and U^{VI} surface complexation on kaolinite in the presence of humic acid and CO_2 (e.g., Krepelova et al.¹¹⁶).

Interaction of Actinides with Microbial Organisms. Microorganisms are generally present at most actinide-contaminated sites, often bound to mineral surfaces by extracellular polymeric substances in the form of biofilms, and can impact the speciation of actinides, particularly their oxidation states. Actinides have no biological utility to microorganisms other than serving as potential terminal electron acceptors; however, when attached to cell-wall metal-binding sites, actinides could interfere with essential element uptake and utilization and alter cell metabolism (see Lovley et al.,¹⁴⁹ Neu et al.,¹⁵⁰ and Lloyd¹⁵¹). The interaction of actinides with the surfaces of microbial organisms has been reviewed by Antonio and Soderholm,¹¹¹ Reed et al.,¹⁴ and Runde and Nue.¹² Here we discuss the types of functional groups present in the outer membrane of Gram-positive and Gram-negative bacteria and the types of microbial processes that can have a profound impact on actinide speciation. In addition, we present several examples of the interaction of actinide species with cell-wall functional groups based on EXAFS spectroscopy studies.

The cell walls of bacteria contain a much wider variety of functional groups than mineral surfaces, including carboxyl, phosphoryl, hydroxyl, amine, imidazol, and sulfhydryl groups.^{152–159} Depending on the solution pH, these functional groups can be protonated or deprotonated, resulting in pH-dependent charges on bacterial cell surfaces. Nonetheless, bacterial cell walls are typically negatively charged at neutral pH and therefore have a high affinity for metal cations, including actinides. Cell-wall functional groups with hard donor atoms, such as carboxylate, phosphonate, sulfonate, and hydroxyl, can

complex hard metal ions, including actinides, resulting in highly stable species. Thus, bacteria have a great potential for strongly binding actinide cations. Because of the high charge and large size of actinide ions, they are more likely to bind to the exterior of cell membranes rather than being transported across them; however, chelation by bacterially secreted siderophores can result in their transport through ion channels due to recognition of siderophore-bound actinides by membrane proteins, resulting in accumulation inside cells. The interactions of actinides with bacterial surfaces can result in their accumulation and transformation into different species, including reduced forms of redox-sensitive actinides due to the reducing conditions of cell surface regions. In addition, dissimilatory metal-reducing bacteria (DMRB) have been found to reduce U^{VI} , Np^V , Pu^{VI} , and Pu^{V} .^{149,160} The reduced species can precipitate as actinide-containing biominerals such as UO_2 and PuO_2 or remain bound to biomass.^{161,162} DMRB can also produce reductants such as Fe^{II} and Mn^{II} , which can reduce higher-valent actinides. In contrast, interactions with bacteria that oxidize actinides lead to more soluble species. Thus, microbial processes can cause both mobilization and immobilization of actinides.

XANES spectroscopy studies of the interaction of the DMRB *Shewanella putrefaciens* with aqueous UO_2^{2+} showed that soluble U^{VI} is reduced to insoluble U^{IV} .¹⁶³ EXAFS spectroscopy studies of U^{VI} sorption^{164,165} and Pu^{VI} sorption¹⁶⁶ on bacterial cell surfaces have shown that they complex with phosphate functional groups preferentially. Other X-ray absorption spectroscopy studies of uranium and plutonium interactions with bacteria include simple model systems, such as the interaction of U^{VI} with *Bacillus sphaericus* cell surfaces and¹⁶⁷ microbial reduction of U^{VI} , and complex model systems, such as uranyl–citrate–goethite *Pseudomonas fluorescens*.⁷³

■ ACTINIDE COLLOIDS AND COLLOIDAL TRANSPORT OF ACTINIDE SPECIES

Colloidal particles (having at least one dimension in the submicrometer size range) and nanoparticles (with at least one dimension of 1–100 nm)¹⁶⁸ can play important roles in the transport of actinides in the environment (e.g., refs 169–173). At the typically low concentrations of actinides in surface waters and groundwaters, sorption of actinide species on nanoparticle/colloid surfaces can determine the actinide's environmental fate.¹² Operationally, there are two types of colloids or nanoparticles in the context of this review: *intrinsic* (i.e., those produced by aggregation of hydrolyzed actinide species) and *natural* (i.e., inorganic or organic colloids produced by weathering in soils). Intrinsic actinide colloids form by stepwise hydrolysis and polymerization processes. Generation of intrinsic actinide colloids is most likely to occur near-field to actinide waste disposal sites, where they can become mobilized and travel to far-field environments.

Pu^{IV} colloid polymers are good examples of intrinsic actinide colloids, which can range in size from one to hundreds of nanometers.¹⁷⁴ The solution concentration of such metastable intrinsic actinide colloids can exceed the thermodynamic solubility of plutonium oxides and hydroxides significantly.^{86,175,176} Although such colloids are relatively stable and are not destroyed by dilution, they can be altered by oxidation of Pu^{IV} . Structural characterization of intrinsic plutonium(IV) colloids by EXAFS spectroscopy^{177,178} revealed structural features characteristic of crystalline PuO_2 . Similar intrinsic colloids of Th^{IV} ¹⁷⁹ and Np^{IV} ¹⁷⁶ have also been found.

Yet another pathway for generating actinide-containing nanoparticles is through reduction of actinyl ions in solution by dissimilatory iron-reducing bacteria such as *S. putrefaciens*. For example, this bacterial species has been found to reduce U^{VI} in solution to uraninite (UO_{2-x}) nanoparticles.¹⁸⁰

A new type of intrinsic Np^V solution colloid that involved cation–cation interactions (i.e., with the oxygen atom of one actinyl ion bonded to a second actinyl ion, where it is also one of the equatorial edges of the bipyramid around the second actinyl ion) was discovered by Sullivan et al.¹⁸¹ Within the past 7 years, highly complex nanoscale uranyl- and neptunyl-based nanostructures^{182–186} and plutonium oxide clusters⁸⁴ involving cation–cation interactions have been reported. This type of connectivity is a major structural feature of ~50% of the known solid-state structures that contain pentavalent actinides (mostly uranyl and neptunyl) and leads to framework structures as well as chain and sheet structures.¹⁸⁷ In addition to these types of nanoclusters, a new class of uranyl–peroxide (H_2O_2) cage nanocluster based on the bent uranyl– H_2O_2 –uranyl interaction characteristic of the mineral studtite ($[(UO_2)(O_2)(H_2O)_2] \cdot 2H_2O$) is now known, with sizes of ~1.5–3.0 nm and 20–60 uranyl polyhedra.¹⁸⁸ Little is known about the stability and aqueous solubility of actinide nanoparticles exhibiting cation–cation or uranyl– H_2O_2 –uranyl interactions, and they have not yet been discovered in natural or contaminated environments. One recent study has shown that $[Pu_{38}O_{56}Cl_x(H_2O)_y]^{(40-x)+}$ nanoparticles sorb to muscovite basal planes, covering ~17% of the surface.¹⁸⁹ Generation of intrinsic actinide colloids is most likely to occur near-field to actinide waste disposal sites, where they can become mobilized and travel to far-field environments.

Natural colloids consist of many different types of minerals, although the most common are clays, zeolites, carbonates, and iron and manganese (oxyhydr)oxides. Short-range-ordered mineral phases such as ferrihydrite are among the most significant scavengers of uranium, with uranium forming inner-sphere complexes.^{190,191} Sorption of U^{VI} on ferrihydrite in the pH range 5–8 leads to an enrichment factor several orders of magnitude higher than that for other crystalline oxides, silica gels, or clays.^{192,193} Occurring either as mineral coatings or suspended matter, these phases play an important role in radionuclide migration. Natural colloids can also consist of NOM, polyelectrolytes derived from the degradation of plants and animals that contain abundant aromatic carboxylate and phenolate groups that can bind actinide ions.^{75,194}

Natural inorganic colloids can sorb significant quantities of actinides^{81,195–197} because of their large reactive surface areas per unit mass. As a result, they play a major role in actinide mobility in subsurface environments. For example, colloid-facilitated transport of plutonium is responsible for its subsurface movement from the Nevada test site in the western USA to a site 1.3 km south over a relatively short time period (~40 years).¹⁹⁸ In addition, Kaplan et al.¹⁹⁹ found that colloid-facilitated transport of radium, thorium, uranium, plutonium, americium, and curium in an acidic plume beneath the Savannah River, SC, site helps to explain the faster than anticipated transport of these actinides. This study also found that plutonium and thorium are most strongly sorbed on colloidal particles, whereas americium, curium, and radium are more weakly sorbed. EXAFS spectroscopy and synchrotron-radiation-based XRF are now shedding light on how plutonium and other actinide ions sorb on colloidal mineral particles and undergo redox transformations in some cases.²⁰⁰ A recent study

by Novikov et al.¹⁹⁶ found that 70–90 mol % of ²³⁹Pu and ²⁴¹Am in groundwater below the Mayak Production Association site, Urals, Russia, is sorbed on hydrous ferric oxide nanoparticles. At higher plutonium concentrations relevant to near-field conditions, reduction of adsorbed Pu^V to Pu^{IV} results in the formation of intrinsic colloidal PuO₂.¹³⁰ Both studies confirm that colloids are responsible for long-distance transport of plutonium and americium at this site.

■ ACTINIDE-CONTAINING MINERALS

Actinide-bearing minerals are important from two standpoints. First, the mineralogy of spent fuel or the solid-phase waste forms, such as cements, determines its susceptibility to radiation damage, oxidation, and ultimately release of radionuclides to the environment.^{1,2,201} Insight into the stability of immobilized waste forms comes from both laboratory studies^{202–204} and the natural alteration of mineral analogues such as uraninite (UO₂),^{205–210} which is both the dominant uranium ore mineral and the primary form of the fuel in light water reactors. Second, the stabilities of the solid phases that form due to alteration of the original waste package, precipitation from a concentrated waste solution, or in situ reduction may provide important controls on aqueous actinide concentrations. Collectively, both the alteration mineralogy of ore deposits and the precipitated phases at contaminated sites provide insight into the range of solid phases that control actinide mobility.

The primary U^{IV}-bearing minerals include uraninite, which can be generalized to other actinides as An^{IV}O₂, and coffinite [U(SiO₄)_{1-x}(OH)_{4x}], which is isostructural with zircon (ZrSiO₄) and thorite (ThSiO₄) (Figure 8).^{211,212} The release of uranyl due to oxidative dissolution of uranium(IV) oxides

and uranium(VI) silicates can result in precipitation of a large range of secondary hydrous uranyl minerals depending on the composition of the solution. The near-neutral range of pH is also associated with the lowest solubilities of U^{VI}, resulting in a common alteration sequence starting with the formation of oxide hydrates followed by uranyl silicates or phosphates.^{205,207,209,213} Common alteration minerals include oxides and hydroxides such as schoepite (UO₃·1–2H₂O) and becquerelite (Ca[(UO₂)₃O₂(OH)₃]₂(H₂O)₈), carbonates like rutherfordine (UO₂CO₃) and liebigite (Ca₂UO₂[(CO₃)₃]·11H₂O), silicates like uranophane (Ca[(UO₂)(SiO₃OH)]₂(H₂O)₅) and soddyite [(UO₂)₂SiO₄·2H₂O], and phosphates such as autunite (Ca[UO₂PO₄]₂·10–12H₂O).

Various uranium minerals have been found to be important controls on the speciation of actinides at contaminated sites. For example, at the Hanford, WA, site, uranyl silicates (uranophane) exist within microfractures of quartz and feldspar grains.^{93,214,215} Beneath the Hanford 300 Area ponds, uranium was found to be incorporated in calcite and precipitated as metatorbernite [Cu(UO₂PO₄)₂·8H₂O] and cuprosklodowskite [Cu(UO₂)₂(SiO₄)(H₃O)₂·2H₂O]. Discrete uranyl phosphate phases have also been observed at the Oak Ridge, TN, site.^{133,216} Various sensitive spectroscopic approaches have been used to identify the uranium minerals in these settings, including X-ray absorption spectroscopy and micro-X-ray diffraction,⁹³ micro-XANES spectroscopy,²¹⁴ and laser fluorescence spectroscopy.^{215,217}

To date, over 360 structures containing U^{VI} have been identified, and some of these may incorporate other actinides and radionuclides.^{211,212} Because the uranyl ion is usually coordinated by four, five, or six oxo groups, the axial oxygen atoms form the apexes of square, pentagonal, or hexagonal bipyramids, while the coordinating oxo ions bond to two or three neighboring uranyles. The resulting polymerization, which is reduced by the presence of OH⁻ or H₂O, facilitates a hierarchical structural classification of U^{VI} minerals according to their anion topology and whether or not they form infinite sheets (e.g., schoepite/becquerelite, rutherfordine, uranophane, soddyite, and autunite), finite clusters (e.g., liebigite), infinite chains, or isolated polyhedra.²¹² Sheets of polyhedra are by far the most common structural units, and they are often linked through low-valence cations or hydrogen bonds or in some cases through anions, resulting in a framework-like structure.²¹² Figure 8 shows examples of the anion topologies for the square-, pentagonal-, or hexagonal-bipyramidal polyhedra and for different interlayer linkages and other polyhedra, such as silicate, carbonate, and phosphate.

The structures of the U^{VI} minerals also determine the extent of incorporation of other actinides and radionuclides. Most actinides, because of variable oxidation states, cannot substitute directly for uranyl or would require a charge-coupled substitution. For example, although NpO₂⁺ is geometrically similar to the uranyl ion, other substitutions must occur elsewhere in the structure to maintain charge balance. In general, structures with interlayer cations, such as becquerelite and uranophane, have been shown to incorporate more neptunium than structures with neutral sheets and interlayers.^{211,218,219} Continued investigation and experimentation regarding the incorporation of actinides and other radionuclides (such as ¹³⁷Cs, ⁹⁰Sr, etc.) into uranium minerals and other secondary phases will improve efforts to manage and predict the actinide mobility in near-field sites. Although uranium is

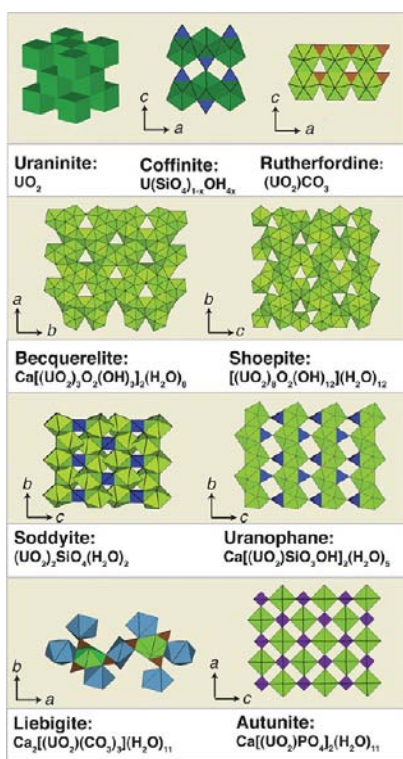


Figure 8. Polyhedral representations of common uranium-containing minerals formed in different environments (modified from Burns et al.^{188,201}). Polyhedral corners are defined by oxygen-atom positions.

often more prevalent in the environment in terms of concentration, the activities of neptunium, plutonium, and americium are likely to be much higher. The coprecipitation and incorporation of actinides into other secondary minerals are also important sequestration processes, as discussed in previous sections.

■ SPECIATION OF URANIUM AT U.S. DOE FIELD SITES

Although a great deal of knowledge has been gained from the study of carefully controlled model systems, contaminated field sites exhibit extensive physical, chemical, and hydrological complexity. Recent advances in microspectroscopic methods have improved our ability to characterize small samples at the nano- to microscale, resulting in new discoveries about the speciation and mobility of actinides in complex environments. At the same time, many model predictions for remediation outcomes are typically based on highly simplified models that have proven to be incorrect. Further combined model system–field system studies, particularly in the areas of microbially driven redox transformations and abiotic sequestration mechanisms, are needed. The sections below provide details from a number of recent studies on the speciation, transport, and remediation of uranium and plutonium at a number of U.S. DOE field sites that have attracted much public and scientific attention over the past several decades.

■ URANIUM SPECIATION AT HANFORD, WA

The Hanford site, within the Hanford/U.S. DOE Nuclear Reservation in eastern Washington State, USA, was the primary plutonium production facility for the U.S. DOE between 1943 and 1989. Nine nuclear reactors along the Columbia River were operated to produce plutonium from the fission of uranium fuels, and a range of intensive processing recipes was used to concentrate the product plutonium, resulting in large volumes of radioactive waste of varied compositions.²²⁰ Contamination by uranium and other actinides (see, Felmy et al.⁷⁹ for a discussion of plutonium contamination) thus includes leaks or spills beneath waste storage tanks in the 200 Areas, process ponds in the 300 Area, and smaller-scale contamination from cribs and trenches in both the 200 and 300 Areas (Figure 9).²²¹

The Hanford site sediments are predominantly unconsolidated with considerable heterogeneity, low organic matter content, and low microbial activity.²²² In the central plateau of the 200 Areas, the sediments are thick and the depth to the water table is between 60 and 80 m, and thus the majority of the contamination resides within this thick vadose zone (the coarse-textured sands are typically less than 30% water-saturated) where infiltration rates are between approximately 0 and 30 mm/year.^{223–225} At the 300 Area in the southeast section of the Hanford site, approximately 100 m from the Columbia River, process effluent storage ponds were located within a shallow vadose zone.^{226,227} Fluctuations in the stage of the Columbia River result in periodic flushing of this contaminated zone, creating a complex hydrological system.

Because of the ubiquitous presence of detrital and secondary carbonate minerals, the background soil water pH across the site is typically close to 7 and oxic conditions are prevalent.²²⁰ Elevated bicarbonate in the vadose and groundwater zones generally enhances the formation of uranylcarbonato complexes, increasing the solubility of uranium precipitates and reducing the adsorption of uranium on sediment particle

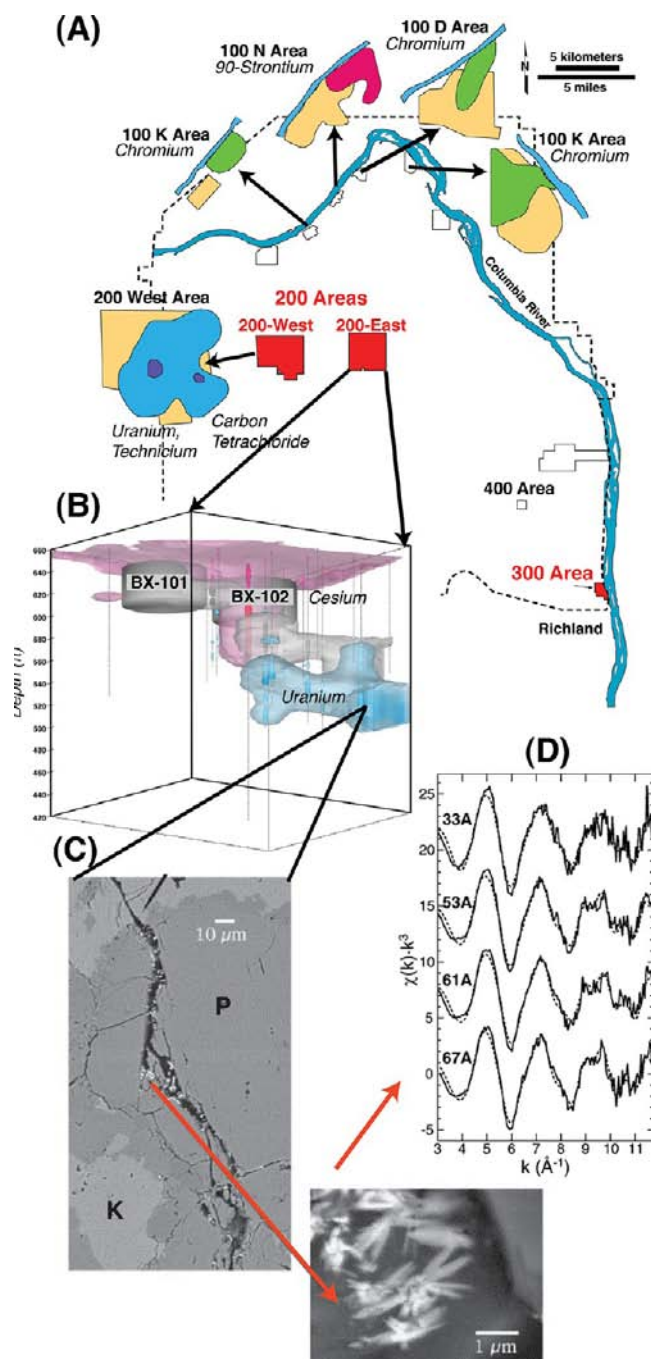


Figure 9. (A) Map of the Hanford, WA, site, showing locations of the 200 and 300 Areas and the contaminant plumes in the vadose zone beneath various Hanford tank farms (not to scale). (B) Lower left side showing the three-dimensional nature of ^{137}Cs , ^{125}Sb , and ^{238}U plumes beneath Tank BX-102 in the 200 East Area, where 300,000 L of waste containing 7–8 tons of uranium was spilled in 1951. (C) Backscattered electron images of vadosed-zone plagioclase grains containing sodium boltwoodite in cracks.²¹⁴ (D) U L_{III} -edge XAFS spectra of sodium boltwoodite grains from Catalano et al.⁹³ (composite modified from Brown et al.³⁰¹).

surfaces. The very stable aqueous $\text{Ca}_2\text{UO}_2(\text{CO}_3)_3$ species^{32,50,228} has been implicated in suppressing U^{VI} (bio-)reduction,^{39,41–43,229,230} diminishing U^{VI} sorption,^{108,109,231,232} and enhancing U^{IV} reoxidation,²³³ under the neutral to alkaline conditions typical at Hanford. Infiltration rates and unsaturated zone hydraulic conductivities are also extremely important for

controlling the uranium mobility and distribution because low permeability zones within the sediment may retain high uranium concentrations, whereas rapid flow rates result in minimal retardation of uranium.^{234–236} The following discussion compares two cases of uranium contamination in the 200 and 300 Areas, respectively, in order to illustrate how the original waste–rock interactions and the physical distribution of uranium-bearing phases are closely coupled with the ultimate speciation and mobility of uranium.

Hanford 200 Area. A total of 67 of the 149 single-shell tanks containing high-level radioactive waste at the Hanford site are listed as known to have or suspected of having leaked during their operational lifetime.^{237–239} The B, BX, and BY tank farm complex located in the 200 East Area contains waste solutions from the plutonium–uranium plant. Nearly half of the tanks in this complex have confirmed or suspected leakage. The composition and volume of waste lost from many of these tanks are uncertain. Tank BX-102 is exceptional in that its leakage was fairly well documented.²⁴⁰ An estimated 7000–8000 kg of U^{VI} was discharged to the vadose zone in the BX tank farm as a result of a single overflowing event at Tank BX-102 in 1951. This “metal waste solution” had a pH of approximately 10, contained 0.5 M U^{VI}, 2.5–5.0 M Na₂CO₃, and 0.36 M phosphate, and included virtually all fission products.²⁴⁰ Portions of this plume have reached the groundwater table (~80 m below), resulting in groundwater with uranium concentrations elevated above the maximum contaminant level (MCL) of 30 µg/L.²⁴¹

Recent studies conducted on vadose-zone sediments of a borehole beneath the BX-102 tank^{93,217,242,243} have provided valuable information linking the molecular-level speciation to the uranium mobility observed within this plume (Figure 9). Laser fluorescence speciation of uranium in pore waters from two BX-102 core samples indicates the predominance of UO₂(CO₃)₃⁴⁻ and possibly Ca₂UO₂(CO₃)₃.²⁴⁴ Solid-phase uranium precipitates in the BX-102 core are the uranyl silicate (uranophane) group, predominantly sodium boltwoodite [Na(UO₂)(SiO₃OH)·1.5H₂O], precipitated within microfractures of quartz and feldspar grains.^{93,214,217} Uranyl is also present as adsorbed species on phyllosilicates. Additional EXAFS studies of uranyl adsorption/desorption on chlorite, a common iron-bearing phyllosilicate at Hanford, further determined that up to 70% of the uranyl is present as weakly sorbed surface complexes,³⁷ which could help to explain the continuing release of uranium into the plume at this site. However, because a substantial fraction of the uranyl silicates precipitated within the intragrain fractures of the primary minerals, slow dissolution kinetics of these uranium(VI) silicates from micropores within sediment grains and intragranular diffusion-limited mass-transfer keep rates of U^{VI} release into pore waters relatively low.^{242,245} Molecular dynamics simulations have shown that the nanopores or nanofractures within a feldspar grain also reduce the diffusivity of uranyl complexes, further inhibiting mass transfer.²⁴⁶

Experimental approaches have also been used to simulate the spilling event using reconstructed waste solution followed by aging in contact with Hanford sediments at 70 °C.^{236,247} These experiments suggest that the formation of uranium-bearing colloids of variable composition can occur at the leading edge of the plume as the pH was neutralized.²³⁶ Low permeability zones also strongly retained uranium. After aging of the sediments, the aqueous uranium concentrations decreased because of intragranular diffusion and precipitation of various

uranium-bearing minerals, many of which were not previously detected in borehole studies.²⁴⁷ The uranium solid phases have distinctly different mineralogy depending on their location along the plume path and distribution within microveins of sediment.²⁴⁷ Finally, this study confirmed the importance of the aqueous uranylcarbonato complexes [UO₂(CO₃)₃⁴⁻] within the plume body and Ca₂UO₂(CO₃)₃ in the plume front in facilitating the transport of uranium to the groundwater during gravity-driven migration of the residual waste solution.

Hanford 300 Area. A large body of uranium-contaminated sediments resides in close proximity to the Columbia River at the 300 Area in the southeast section of the Hanford site at the former location of two process effluent storage ponds (the “North and South Area Process Ponds”)^{226,227} (Figure 9a). Estimated quantities of uranium disposed of between 1943 and 1975 into the process ponds range from 33,000 to 59,000 kg. In contrast to the alkaline uranium waste solutions associated with the 200 Area storage tanks, the 300 Area waste ponds received acidic uranium(VI)–copper(II) nitrate (with an approximate 10:1 Cu-to-U ratio) and basic sodium aluminate waste streams, among many other forms of wastes and debris. The pH of the pond water varied from 1.8 to 11.4, and sodium hydroxide was frequently used to minimize leaching of copper and uranium through the vadose zone.²²¹

In 1996, 640,000 tons of contaminated sediments were removed from the ponds, and an additional meter of sediment was removed from 2001 to 2002. Although the most highly contaminated sediments were excavated and removed, uranium contamination continues to extend through the underlying vadose zone and into the shallow aquifer that drains into the Columbia River. The groundwater uranium concentrations have remained at or only slightly below pre-1996 levels, with minimal attenuation; the current 300 Area groundwater plume reaches uranium concentrations in excess of 100 µg/L.²⁴⁸

Samples within the uranium plume at the 300 Area, collected from the current land surface through the vadose zone to the groundwater, have been studied intensively.^{220,227} Spectroscopic analyses of sediments excavated from under the former 300 Area ponds found uranium contained in solid phases via coprecipitation with calcite at shallow depths and precipitated as metatorbernite [Cu(UO₂PO₄)₂·8H₂O] and cuprosklodowskite [Cu(UO₂)₂(SiO₄)(H₃O)₂·2H₂O] at intermediate depths (Figure 10).²⁴⁹ Approximately 1% of the contaminant uranium occurs as grain coatings on large cobbles and clasts (2–8 mm diameter), whereas the remainder of the uranium is contained within the silt and clay fraction (<53 µm), which comprise as little as 2% of the total sediment mass.²⁵⁰ Recent work has shown that native bacterial populations may enhance the release of U^{VI} from uranyl phosphate minerals.²⁵¹ In the deeper vadose zone and groundwater, U^{VI} was predominantly sorbed onto phyllosilicates, although sorbed uranium was also an important U^{VI} reservoir at the intermediate depths.^{94,226,249,252} The multiple reservoirs of uranium with different stabilities and release kinetics pose a challenge for remediation efforts in the 300 Area, particularly monitored natural attenuation (MNA), because the solids provide a long-term source of uranium to groundwater, while the sorbed fraction represents an intermediate storage reservoir between the more stable solids and the groundwater.^{253,254}

Collectively, studies of uranium speciation at the Hanford/U.S. DOE site indicate the importance of both the composition and physical distribution of secondary mineralization that arises through interactions between percolating waste and host

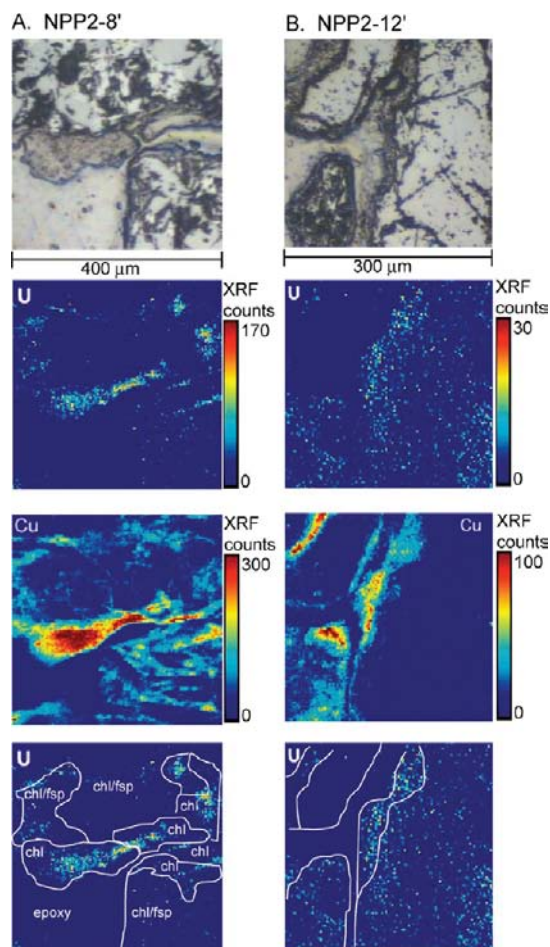


Figure 10. Reflected light images and synchrotron XRF U $L\alpha$ and Cu $K\alpha$ maps of Hanford 300 Area NPP2 sediments. Grain boundaries on the uranium map are outlined in white based on the reflected light images, and the mineral phase identification is based on the μ -XRD patterns. The phases present are chlorite (chl), feldspar (fsp), metatorbernite (mtb), amorphous phases (am), and epoxy.⁹⁴

sediments. At the 200 Area, isolated uranyl silicate phases formed from the silicon-poor alkaline wastes in diffusion-limited cracks in mineral grains, creating a more stable reservoir of uranium in the subsurface under the relatively low flow rates of the unsaturated zone. In contrast, within the 300 Area, the acidic copper-laden waste resulted in the formation of several uranyl-bearing solid phases distributed as diffuse mineral coatings and in intragranular cracks, along with adsorption of uranium onto phyllosilicates, creating multiple reservoirs of uranium with different mobilities and release rates.²⁵³ The periodic flushing of the sediments by groundwater continues to mobilize uranium, resulting in a persistent uranium plume. Collectively, the presence of the different U^{VI} reservoirs (e.g., adsorbed vs solid phase) with different release kinetics hindered efforts to predict the fate of U^{VI} within the vadose zone and its transport to groundwater and subsequently to the Columbia River. Detailed studies of the speciation and transport of uranium such as those discussed above have greatly improved the conceptual models for uranium transport both at Hanford and across other sites with similar histories.

■ URANIUM SPECIATION AT RIFLE, CO

The Old Rifle ore-processing site is one of two uranium-contaminated sites located in the town of Rifle, in northwestern Colorado, USA. This site hosted a vanadium and uranium mill that operated between 1924 and 1958.²⁵⁵ Uranium contamination in the aquifer was derived from mill tailings. Unlike the Hanford and Oak Ridge sites, which are still being cleaned up under the Comprehensive Environmental Response, Compensation and Liability Act (CERCLA), the DOE-EM cleanup and removal of tailings and other contaminated surface materials at Old Rifle were completed by 1996 under Title I of the Uranium Mill Tailings Radiation Control Act of 1978. Subsequently, Old Rifle has been managed by the U.S. DOE Office of Legacy Management (DOE-LM). In spite of being “cleaned up”, uranium contamination persists in the aquifer at concentrations up to 1.5 μ M,²⁵⁶ indicating that the aquifer sediments themselves have become a secondary source of contamination. A single plume of about 675 m long and 225 m wide and containing an estimated 259,000,000 L of contaminated groundwater exists at the site (Figure 11).²⁵⁷ The plume

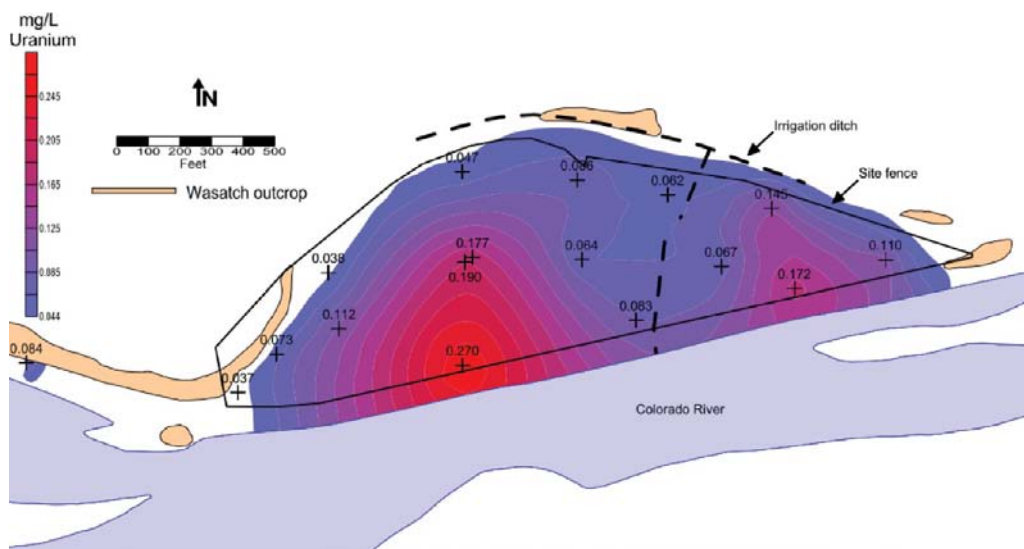


Figure 11. Uranium distribution in the Old Rifle aquifer, May 1998.²⁵⁷

discharges into the Colorado River at the down-gradient portion of the site. The aquifer itself is shallow, up to 8 m thick of which about 3 to 4 m is permanently saturated, and composed of cobble, gravel, and sand lithic fragments derived from the Rocky Mountain Front Range, with the uppermost 2 m being a clay cap.²⁵⁸ Sediments are dominated by quartz and feldspar and contain lower abundances of amphibolites and clay. The clay fraction contains smectite, kaolinite, and chlorite, with illite being dominant.¹⁶¹ The Old Rifle site shares aquifer, lithology, and geochemical characteristics with many of the other contaminated DOE-LM sites in the Colorado River basin and hence serves as a model for these other sites. The Old Rifle site is the location of the Rifle Integrated Field Research Challenge (IFRC) project. The Rifle IFRC has been studying microbial ecology and biogeochemical cycling of uranium during electron-donor amendment to the aquifer for the purposes of researching bioreduction as a means to remediate uranium contamination.²⁵⁶ In addition to uranium, contaminants of concern at the Old Rifle site include arsenic, selenium, and vanadium.²⁵⁵ Field-scale research at the site is now focusing on the extant microbial metabolic potential of the site and its relationship to carbon cycling in addition to metal and radionuclide contamination.

The Old Rifle aquifer exhibits naturally low dissolved oxygen (DO; <1 mg/L, with some anoxic wells), ~8 mM SO_4^{2-} , Ca^{2+} , and HCO_3^- (the latter in near equilibrium with calcite). The primary aqueous species of uranium in Rifle groundwater are uranium(VI) carbonate and calcium–uranium(VI) carbonate ternary species.^{259,260} Consequently, uranium transport at the site is dominated by advection of U^{VI} in groundwater. Adsorption of U^{VI} on mineral surfaces is believed to be the primary mechanism of U^{VI} retardation.²⁶¹ Sediment uranium concentrations are typically <1 mg/kg, which is too dilute for most mineralogical characterization techniques. Consequently, the identities of phases controlling uranium groundwater concentrations are not known. Given the variability of uranium concentrations across the plume, a single dominant control is unlikely. However, Cerrato et al.²⁶² recently noted that uranium groundwater concentrations at the Old Rifle site are in the range expected for the solubilities of liebigite, $\text{Ca}_2\text{UO}_2(\text{CO}_3)_3(\text{H}_2\text{O})_{10}$, and becquerelite, $\text{Ca}(\text{UO}_2)_2\text{SiO}_3(\text{OH})_2 \cdot 5\text{H}_2\text{O}$. The Old Rifle aquifer also contains numerous thin lenses of fine-grained organic-rich sediments in which metals, including iron and uranium, and sulfur have been naturally reduced to U^{IV} , ferrous, and sulfidic compounds.¹⁶¹ Indigenous bacterial communities that couple the oxidation of sediment organic carbon to metal and sulfate/sulfur reduction are implicated as the reducing agents in these sediments. Uranium diffusing into these naturally reduced zones is reduced to monomeric U^{IV} species. These species have relatively low solubility, and hence uranium accumulates in the sediments, resulting in concentrations as high as 50 mg/kg, i.e., orders of magnitude higher than the surrounding ambient aquifer sediments. Slow release of uranium from these zones is suspected to be an important mechanism contributing to plume persistence.

The primary contaminant mitigation technique selected for 1207 the Old Rifle aquifer is MNA, where natural flushing of the aquifer by groundwater desorbs, dilutes, and effluxes uranium into the Colorado River. This approach was projected to reduce uranium groundwater concentrations in the Old Rifle aquifer to levels below the MCL (30 $\mu\text{g}/\text{L}$) within one decade.²⁵⁷ This strategy has proved ineffective, a result

observed at other DOE-LM sites in the Colorado River basin.²⁶³ Alternative mitigation strategies are under consideration, but a final solution has not yet been identified. Stimulated bioremediation, i.e., injection of soluble organic carbon into the aquifer to induce microbial reduction of U^{VI} to U^{IV} , is unlikely to be chosen as a replacement.

The microbial ecology and biogeochemical cycling of uranium during electron-donor amendment to the aquifer has also been investigated as part of the Rifle IFRC.²⁵⁶ These studies demonstrated that acetate amendment of the aquifer is followed by the development of iron-reducing conditions dominated by *Geobacter* spp.^{259,264} and subsequently by sulfate-reducing conditions in which predominant communities included bacteria related to *Desulfosporosinus* and *Desulfobacteraceae*. Novel microorganisms from candidate divisions BD1–5, OP11, and OD1 have also recently been recovered from groundwater samples collected during biostimulation.²⁶⁵ U^{VI} is rapidly removed from groundwater under metal-reducing conditions.^{259,264} *Geobacter* spp was linked to uranium reduction and found to oxidize acetate even under “deep” sulfate-reducing conditions.²⁵⁶ However, the long-term efficacy of uranium removal may be limited by competing biogeochemical effects such as increases in alkalinity driven by the metabolic activity of sulfate-reducing organisms, which causes adsorbed U^{VI} to desorb. However, if sufficiently high concentrations of acetate are added (10 mM), then prolonged uranium removal can be achieved.²⁶⁵

■ URANIUM SPECIATION AT OAK RIDGE NATIONAL LABORATORY (ORNL)

ORNL, located in east-central Tennessee, USA, is the site of uranium contamination cleanup under the CERCLA of 1980. Remediation activities are being conducted by DOE-EM. Nuclear materials fabrication at Oak Ridge since the 1940s generated large quantities of subsurface uranium contamination. One of the most contaminated of these areas is the Y-12 plant, where 320,000,000 L of highly acidic (pH 1–4) uranium-bearing process effluent was discharged to four shallow unlined “S-3” ponds between 1951 and 1983 (Figure 12).²⁶⁶ Discharged liquids contained relatively high concentrations of NO_3^- (<74,000 mg/L), Ca^{2+} (<3000 mg/L), Al^{3+} (<4800 mg/L), and U^{VI} (<300 mg/L), as well as volatile organic compounds.²⁶⁶ Seepage of fluids into the aquifer over the 32-

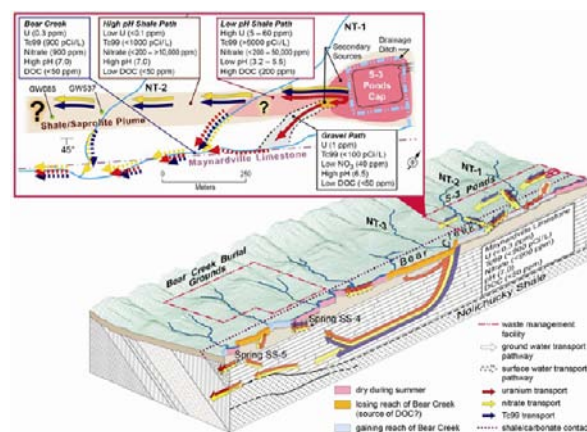


Figure 12. Major source zones and flow paths for uranium, nitrate, and technetium in the Bear Creek Valley watershed, which encompasses the ORNL FRC (from http://public.ornl.gov/orifc/orifrc3_site.cfm).

year lifespan of the ponds resulted in contamination of sediments and bedrock and creation of a large secondary contaminant source. Slow release of uranium from these subsurface materials into groundwater sustains a 4-km-long uranium groundwater plume, which discharges into Bear Creek as well as the underlying porous karstic limestone.^{267,268} The Y-12 area is the location of the Oak Ridge Field Research Center, which has conducted extensive investigations of uranium biogeochemistry and transport in the Y-12 subsurface. This work has shown that reaction of the acidic pond fluids with carbonate minerals in the saprolite (weathered bedrock retaining the fabric and structure of the parent rock) and shale around the ponds partially neutralized waste fluids and allowed them to acquire dissolved inorganic carbon. The pore water pH varies from 3.5 in areas adjacent to the S-3 pond locations to ~ 7 in more distant areas.^{269–271} Uranium pore water and sediment concentrations attain surprisingly high values, up to 280 μM and 800 mg/kg, respectively. Waste inputs to the S-3 ponds were halted in 1983, and the ponds were neutralized and bionitrified. Pond water subsequently was pumped away and treated, and the ponds were filled with sediment and capped with a parking lot to minimize infiltration by groundwater.²⁶⁶

Uranium behavior in the Y-12 plant subsurface is mediated by aqueous complexants, particularly bicarbonate anion, oxidants, pH, and the chemical and physical properties of the compositionally and structurally complex sediment matrix. DO is typically 1–4 mg/L, although suboxia (< 1 mg/L DO) occurs in the deeper and more highly contaminated locations in the aquifer.²⁷¹ Uranium generally occurs in the 6+ oxidation state in Y-12 groundwater.²⁷² Bicarbonate concentrations of 10–32 mM are common.^{266,273} Y-12 plant groundwater also contains up to 29 mM dissolved Al^{3+} , similar concentrations of Ca^{2+} and Na^+ , millimolar concentrations of K^+ and Mg^{2+} , and up to 227 mM nitrate.^{269–271} The abundant HCO_3^- , Ca^{2+} , and Na^{2+} dictate that the dominant U^{VI} aqueous species in Y-12 groundwater are $\text{Ca-U}^{\text{VI}}\text{CO}_3$ and $\text{Na-U}^{\text{VI}}\text{CO}_3$ complexes.²⁷² Neutralization of the groundwater results in the precipitation of iron(3+) oxides and Ca^{2+} and Al^{3+} -bearing phases,^{274,275} which can clog aquifer pore spaces.

Y-12 subsurface sediments are composed of saprolite and interbedded sandstone and shale bedrock. Both the saprolite and less-weathered bedrock contain quartz, calcium feldspar, mica, clays, and iron/manganese oxides^{271,276} and are highly jointed and fractured. Fractures generally are filled with calcite, clays, and iron/manganese oxides. However, a more porous transition zone of ~ 2 –3 m thickness lies at the base of the unconsolidated sediment and above more competent bedrock. Acidic groundwater has dissolved calcite veins in this zone, resulting in yet greater porosity and higher hydraulic conductivity than the surrounding matrix. Consequently, the transition zone acts as a conduit for contaminant transport, and the highest concentrations of uranium, nitrate, and other contaminants are found in this location.²⁷¹ Preferential groundwater flow in fractures has resulted in weathering of the surrounding shale into thin (< 25 cm) iron oxide rich claylike seams exhibiting spongelike internal porosity at the scale of tens of micrometers. These structures strongly retain uranium. Elsewhere, sediment voids and joint surfaces are coated with clays (illite, kaolinite, and vermiculite), goethite, ferrihydrite, manganese oxides, and quartz.^{133,271} In the most contaminated sediments, the highest uranium concentrations occur in clay bands that also contain black, reduced iron

oxides.²⁷¹ Electron microscopy and energy-dispersive spectroscopy studies have shown that uranium is generally associated with phosphorus, implying an important role for phosphate as a complexant of U^{VI} . Uranium and phosphorus are associated with mineral hosts, particularly iron and iron/manganese oxides with uranium contents estimated in the 0.1 wt % range. Uranium and phosphorus are also associated with aluminum oxides or as discrete uranyl phosphate phases.^{133,216} In more highly weathered low-pH sediments, there is less association of uranium to iron and aluminum oxides. EXAFS spectroscopy measurements, which complement electron microscopy studies by providing information on bulk-scale uranium speciation, indicate that U^{VI} is associated dominantly with both phosphorus and carbon in sediments at mineral surfaces or bound to organic matter. A small fraction of U^{VI} was reported to be present in an oxide-like form.²⁷⁷ Elsewhere in the S-3 pond vicinity, uranium(VI) carbonate precipitates have been observed on dolomitic gravel fill.²⁷⁸

The mineralogy and physical structure of the weathered subsurface materials have profound implications for uranium movement at the site. The abundant clays and iron and iron/manganese (oxyhydr)oxide coatings, which have a high affinity for U^{VI} , play a central role in retarding U^{VI} transport.²⁷⁹ Partial reduction and recrystallization of these iron (oxyhydr)oxides are implied by the presence of black iron (oxyhydr)oxide layers as well as by direct electron microscopy measurements.^{133,271} Recrystallization of iron oxides in the presence of uranium provides a mechanism to account for the apparent incorporation of U^{VI} in goethite and ferrihydrite in the Y-12 subsurface.¹³² The extensive diffusion-limited internal porosity of the weathered saprolite and bedrock also provides a large reservoir that can store and slowly release U^{VI} back to the aquifer.²⁸⁰

Uranium mitigation strategies that have been investigated at the Oak Ridge site include zerovalent iron-permeable reactive barriers.²⁸⁰ A pilot-scale test showed that groundwater flowing through the barrier exhibited dramatically reduced concentrations of uranium and nitrate. However, extensive precipitation of carbonates, sulfides, and iron (oxyhydr)oxides in the barrier pore spaces raises concerns about decreasing permeability and the long-term viability of the barriers. The Oak Ridge FRC also has extensively investigated bioreduction of U^{VI} in the Y-12 aquifer following injection of electron donors (ethanol, glucose, and acetate) to stimulate metal- and sulfate-reducing bacteria that also can reduce U^{VI} to U^{IV} .^{270,281–283} Amendment of the Y-12 aquifer initially led to bacterial denitrification, followed by the establishment of metal- and sulfate-reducing bacterial communities (including *Geobacter* spp, *Anaeromyxobacter* spp, and *Desulfovibrio* spp), reduction of U^{VI} , and a decrease in U^{VI} groundwater concentrations to submicromolar levels. However, reintroduction of DO upon cessation of donor amendment was accompanied by a rapid rebound in dissolved U^{VI} concentrations, suggesting that sustained amendment will be necessary for this technique to be viable. Recently, controlled base addition to precipitate aluminum hydroxides has also been investigated as a potential remediation technique.^{275,284} Laboratory studies have shown that this technique can strongly decrease U^{VI} concentrations in solution, and this behavior has been attributed to the formation of surface complexes of U^{VI} on aluminum hydroxides.

■ URANIUM POLLUTION IN SOILS FROM THE FERNALD, OH, URANIUM PROCESSING PLANT

Uranium pollution in soils at the Fernald, OH, Uranium Processing Plant was studied using molecular spectroscopic and μ -XANES mapping methods.²⁸⁵ Attempts to remediate this soil by carbonate-washing methods, which remove sorbed uranyl ions from mineral surfaces because of the formation of highly stable uranylcarbonato solution complexes above pH 7 (Figure 6), resulted in incomplete removal of the uranium from the polluted soil. An XAFS study by Morris et al.²⁸⁶ identified an insoluble U^{IV} -containing phase in addition to the soluble uranyl species, which explained the ineffectiveness of the remediation methods that were used. These molecular-level studies illustrate the major benefit of understanding the species of a pollutant present at a polluted site prior to choosing a particular remediation technology for its removal. Although these polluted soils were eventually dug up and transported to an EPA-approved disposal site, modification of the soil washing methods could have resulted in effective "in situ" removal of the uranium in this case.

■ REMEDIATION OF URANIUM-CONTAMINATED GROUNDWATER AT FRY CANYON, UT

The Fry Canyon site, which is located along spring-fed perennial Fry Creek in southeastern Utah's White Canyon Mining District, is one of more than 25,000 abandoned mine sites in the western USA.²⁸⁷ Uranium ore upgrading operations conducted at the site between 1957 and 1960 generated 36,000 tons of uranium-bearing sand tailings. Uranium from the tailings subsequently has seeped into groundwater, generating dissolved uranium concentrations in excess of 80 μ M in some locations.²⁸⁸ The tailings were heap-leached to extract copper between 1962 and 1968, and subsequently the site fell into disuse. The U.S. EPA designated the Fry Canyon site for "no further remedial action planned" in 1990. Site groundwater is derived from infiltration of Fry Creek streamwater into the aquifer at the up-gradient end of the site. Contaminated groundwater discharges back into Fry Creek at the down-gradient end of the site. Aquifer sediments are composed of silt to gravel-size fragments derived from nearby sandstone and shale. The aquifer at this semiarid location shares some characteristics with that at Old Rifle, CO. Like Old Rifle, it is shallow (up to 5.5 m thick with the water table located at \sim 2.5 m below the ground surface), and groundwater exhibits near-neutral pH and millimolar concentrations (<10 mM) of SO_4^{2-} , Ca^{2+} , and HCO_3^- .^{289,290} DO is variable at the Fry Canyon aquifer, ranging from \sim 0.4 to 7 mg/L. The aqueous speciation of uranium in Fry Canyon groundwater is expected to be dominated by calcium-uranium(VI) carbonate complexes. Advection of these complexes is expected to be the dominant transport mechanism in the aquifer, whereas adsorption of uranium species on grain surfaces is believed to be an important attenuation mechanism.²⁸⁹

Because of its similarity to other abandoned sites, its accessibility, climate, and aquifer characteristics,²⁸⁹ Fry Canyon was selected as the site of a permeable reactive barrier (PRB) field demonstration project to assess the efficacy of this technology for treating uranium-contaminated groundwater. In their simplest form, PRBs consist of trenches dug through the aquifer to intercept groundwater flow and filled with reactive materials that can sequester uranium while maintaining good hydraulic conductivity.²⁹¹ Key advantages of PRBs include their

reliance on groundwater flow instead of active pumping, low maintenance requirements, and, ideally, relatively favorable ratio of groundwater residence time relative to characteristic rates of desired reactions. Three PRBs were installed at Fry Canyon in 1997, each measuring 2.1 m long by 0.9 m wide and extending to the base of the aquifer.²⁸⁹ One barrier was filled with pelletized hydroxyl apatite [$Ca_5(PO_4)_3OH$] in the form of bone charcoal, which was used without mixing or dilution in aquifer sediments. Another of the PRB trenches was filled with pelletized metallic iron without mixing/dilution with sand or sediments. The third PRB was filled with a mixture of amorphous ferric oxide (AFO) and gravel. These materials were selected following laboratory evaluation^{289,292} to assess the efficacy of the following three sequestration mechanisms: (1) precipitation of relatively insoluble uranium(VI) phosphate solids such as autunite [$Ca(UO_2)_2(PO_4)_2 \cdot 10H_2O$] in the bone char PRB, (2) reduction of U^{VI} to U^{IV} coupled to oxidation of Fe^0 to Fe^{III} in the metallic iron PRB, and (3) adsorption of U^{VI} onto high-surface-area ferric oxide in the AFO barrier. After the 1130-day demonstration period, all three barriers were found to have attenuated groundwater U^{VI} concentrations. The metallic iron PRB was most efficacious over the test period, removing on average of 99.3% of influent uranium. The bone char PRB was least effective, removing on average of 59% of influent uranium.²⁸⁸

The study of the bone-char-barrier-filled material before and after reaction in the Fry Canyon aquifer²⁹²⁻²⁹⁴ presents an interesting example of the use of XAFS spectroscopy and synchrotron radiation powder diffraction to evaluate a uranium remediation strategy. The hypothesis tested in this study was that phosphate anion released by dissolution of the bone char material would react with dissolved U^{VI} to precipitate relatively insoluble autunite. Laboratory studies in which U^{VI} solutions were contacted with synthetic apatite or the bone char fill material showed that chernikovite [$H_2(UO_2)_2(PO_4)_2$] precipitated at relatively high total U^{VI} concentrations (>7000 ppm).²⁹²⁻²⁹⁴ However, at lower U^{VI} concentrations, U^{VI} was found to be adsorbed to the surfaces of the apatite materials, even though the solutions were supersaturated with respect to chernikovite. This behavior indicates that surface complexation reactions are faster and more effective than precipitation under the experimental conditions. In essence, the binding of U^{VI} to apatite surfaces was preventing the formation of the desired solid phase. Sediments cored from the bone char PRB after 540 days of operation contained up to 690 ppm of uranium. Neither XAFS nor XRD results showed any evidence for uranium phosphate precipitates. EXAFS analysis of the reacted bone char showed that the mechanism of U^{VI} attenuation involved sorption of U^{VI} on bone-char surfaces. This finding leads to the prediction that phosphate-based PRBs will become less effective as sorption sites are filled with uranium. Careful monitoring will be necessary to ensure an effective barrier performance and, eventually, restoration.

■ PLUTONIUM POLLUTION IN SOILS AT THE ROCKY FLATS, CO, ENVIRONMENTAL TECHNOLOGY SITE

From 1944 to 1989, the Rocky Flats Plant produced more than 100 tons of plutonium for the manufacture of plutonium pits for U.S. nuclear weapons. This site, comprising 385 acres with 805 buildings and 6000 acres of controlled open space, is located 16 miles from downtown Denver, CO, with a population of almost 3 million people and with over 300,000 people living within the Rocky Flats watershed. During the

decades-long operation of Rocky Flats as a plutonium processing plant, significant pollution of the underlying soils occurred because of spills of processing liquids. There were also several fires that resulted in contamination of concrete in the buildings. Several decades of monitoring showed that 90% of the plutonium was contained in the upper 10–20 cm of soil. Local claims that large amounts of plutonium migrated during spring rain events generated widespread public concern. The risk associated with trace plutonium contamination in soils is controlled to a large extent by its speciation, as discussed earlier. If incorporated in an insoluble phase, plutonium poses less environmental risk because its rate of release will be extremely slow. In contrast, plutonium in readily leachable phases or sorbed weakly on mineral surfaces poses a significant short-term environmental risk. In order to assess the speciation of plutonium in Rocky Flats soils at the 903 drum storage site, LoPresti et al.²⁹⁵ carried out Pu L_{III}-edge XANES spectroscopy studies on soil samples from this site and found that the plutonium was predominantly present as colloidal particles of PuO₂(s), which is highly insoluble under soil water conditions. Similarly, EXAFS spectroscopy studies of the form of plutonium in the contaminated concrete showed that it was also PuO₂(s) (Figure 13).²⁹⁶ This work substantiated earlier

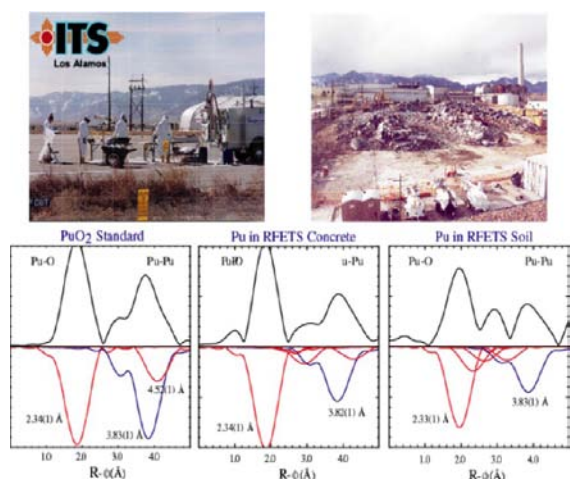


Figure 13. Fourier transforms of Pu L_{III}-edge EXAFS spectra of a PuO₂ crystalline standard, plutonium in Rocky Flats Environmental Technology Site (RFETS) concrete, and plutonium in RFETS plutonium-contaminated soil, showing that the main species of plutonium contamination is crystalline PuO₂. Figure courtesy of D. L. Clark, LANL.

assessments that solute transport models were not applicable to plutonium migration in Rocky Flats soils.^{297,298} Rather, particulate transport was suggested to be the dominant transport mechanism for plutonium migration at the site, although more recent studies suggest that transport of plutonium colloids facilitated by NOM²⁹⁹ or by complexation to biologically produced, cutin-like ligands³⁰⁰ may be more important than transport by purely inorganic colloids. These findings of colloid transport in surface waters translated directly into substantial cost savings because they allowed the remediation contractors to focus efforts on erosion modeling and the construction of dams and barriers to control particulate transport rather than removing huge quantities of soil from the site or implementing very costly soil-washing procedures, which would likely be ineffective because of the insoluble nature of

PuO₂(s). The savings to the U.S. taxpayer was estimated to be in the billions of dollars. Cleanup of this EPA Superfund Site was completed in 2005 (1 year ahead of schedule).²⁹⁸

SUMMARY AND CONCLUSIONS

In light of both the legacy of waste derived from the nuclear fuel cycle and the projected increase in future demand for nuclear energy, continued innovation in the design and implementation of effective remediation of actinides will be an important requirement for securing our energy future. The design of optimal storage vessels to prevent actinide release is another critical management strategy. Innovations in both arenas hinge on our understanding of the intrinsic reactivity of actinides in the environment, from their aqueous speciation, redox kinetics, sorption at mineral surfaces, interactions with microbial organisms and NOM, and incorporation into minerals under different site conditions to their transport as colloids or diffusion to aquifers from microenvironments in the sediments.

In this review, we have highlighted the development of mechanistic information derived from a variety of spectroscopic techniques and the application of such knowledge to quantify and predict microscopic to macroscopic transport behaviors. Across the various contaminated sites we review here and the various remediation strategies employed to clean them up, several key challenges emerge. First, the initial physical and chemical heterogeneity of natural systems often translates into poor predictions of actinide behavior and ultimately the effectiveness of remediation strategies. For example, MNA was of limited utility at both the Hanford, WA, and Old Rifle, CO, sites because of naturally reducing zones or chemical microenvironments, respectively. Both macro- and micro-environments result in slow mass transfer of actinides to the mobile fluid and failure to meet remediation targets but may provide suitable environments for microbially engineered remediation involving direct or indirect reduction or biomineralization. Remediation strategies that involve in situ manipulation of the aqueous speciation or redox state of the actinides, including PRBs, biological reduction, or solvent extraction coupled with pump and treat, are only successful to the extent that they are specifically designed to target aqueous and solid actinide speciation under field conditions. For example, at the Fernald, OH, site, use of carbonate ion to complex uranium as part of a pump-and-treat strategy was unsuccessful because a substantial fraction of the uranium was present as an insoluble U^{IV} phase. Similarly, the success of the plutonium remediation at Rocky Flats can be attributed to the recognition that colloidal transport was the dominant transport mechanism under the site conditions.

On the basis of insight from numerous field and experimental studies, we propose several key areas for future research including (1) continued development of conceptual models of actinide chemistry and testing and evaluation of these models at meso- to macroscopic scales in reactive transport models, (2) research leading to increased understanding of how the intrinsic properties of actinides combined with site-specific conditions control reaction kinetics and pathways and thus their ultimate environmental fate, (3) collection of more information regarding the speciation and redox reactions involving actinides at mineral surfaces, (4) research on opportunities for mineralogical sequestration of actinides, including coprecipitation and trapping in or occlusion by gels and other poorly crystalline phases such as iron (oxyhydr)oxides, and (5) studies

of microbiological processes that immobilize actinides through alteration of the redox state or biomineralization. Decades worth of research into the chemical behavior of actinides provides the critical foundation that makes these research directions possible.

AUTHOR INFORMATION

Corresponding Author

*E-mail: kmaher@stanford.edu.

Notes

The authors declare no competing financial interest.

ACKNOWLEDGMENTS

We thank Forum Guest Editor John Gordon of Los Alamos National Laboratory for inviting us to prepare this review. We also acknowledge support from the Stanford Global Climate and Energy Project (to K.M. and G.E.B.) during the preparation of this review as well as support from the DOE-BER-Subsurface Geochemistry Program through grant BER-DE-SC0006772 (G.E.B.), DOE-BES Scientific User Facilities Division (to J.R.B.), the DOE-BER Science Focus Area grant to SSRL (to J.R.B. and G.E.B.), and NSF Grants EAR-0921134 and EAR-1019894 (to K.M.).

REFERENCES

- Ewing, R. C. *Geosci.* **2011**, *343*, 219–229.
- Ewing, R. C. *Elements* **2006**, *2*, 331–334.
- Abdelouas, A. *Elements* **2006**, *2*, 335–341.
- Macfarlane, A. M.; Miller, M. *Elements* **2007**, *3*, 185–192.
- Goldstein, S. J.; Abdel-Fattah, A. I.; Murrell, M. T.; Dobson, P. F.; Norman, D. E.; Amato, R. S.; Nunn, A. J. *Environ. Sci. Technol.* **2010**, *44*, 1579–1586.
- Ku, T. L.; Luo, S.; Goldstein, S. J.; Murrell, M. T.; Chu, W. L.; Dobson, P. F. *Geochim. Cosmochim. Acta* **2009**, *73*, 6052–6064.
- Wilson, N. S. F.; Cline, J. S.; Amelin, Y. V. *Geochim. Cosmochim. Acta* **2003**, *67*, 1145–1176.
- Allard, T.; Muller, J. P. *Appl. Geochem.* **1998**, *13*, 751–765.
- Allard, T.; Calas, G.; Ildefonse, P. *Chem. Geol.* **2007**, *239*, 50–63.
- Allard, T.; Ildefonse, P.; Beaucaire, C.; Calas, G. *Chem. Geol.* **1999**, *158*, 81–103.
- Choppin, G. R.; Jensen, M. P. Actinides in Solution: Complexation and Kinetics. In *The Chemistry of the Actinide and Transactinide Elements*, 4th ed.; Morss, L. R., Edelstein, N. M., Fuger, J., Eds.; Springer: Dordrecht, The Netherlands, 2010; pp 2524–2621.
- Runde, W.; Neu, M. P. Actinides in the Geosphere. In *The Chemistry of the Actinide and Transactinide Elements*, 4th ed.; Morss, L. R., Edelstein, N. M., Fuger, J., Eds.; Springer: Dordrecht, The Netherlands, 2010; pp 3475–3593.
- Degueldre, C. Identification and Speciation of Actinides in the Environment. In *The Chemistry of the Actinide and Transactinide Elements*, 4th ed.; Morss, L. R., Edelstein, N. M., Fuger, J., Eds.; Springer: Dordrecht, The Netherlands, 2010; pp 3013–3085.
- Reed, D. T.; Deo, R. P.; Rittmann, B. Subsurface Interactions of Actinide Species with Microorganisms. In *The Chemistry of the Actinide and Transactinide Elements*, 4th ed.; Morss, L. R., Edelstein, N. M., Fuger, J., Eds.; Springer: Dordrecht, The Netherlands, 2010; pp 3595–3663.
- Morss, L. R.; Edelstein, N. M.; Fuger, J. *The Chemistry of the Actinide and Transactinide Elements*, 4th ed.; Springer: Dordrecht, The Netherlands, 2010; pp 3475–3593.
- Cowart, J. B.; Burnett, W. C. *J. Environ. Qual.* **1994**, *23*, 651–662.
- Gascoyne, M. Geochemistry of the Actinides and Their Daughters. In *Uranium-Series Disequilibrium: Applications to Earth, Marine, and Environmental Sciences*, 2nd ed.; Ivanovich, M., Harmon, R. S., Eds.; Oxford University Press: Oxford, U.K., 1992; pp 34–61.
- Cowan, G. A.; Adler, H. H. *Geochim. Cosmochim. Acta* **1976**, *40*, 1487–1490.
- Gauthier-Lafaye, F.; Holliger, P.; Blanc, P. L. *Geochim. Cosmochim. Acta* **1996**, *60*, 4831–4852.
- Smellie, J. *Radwaste Mag.* **1995**, *2*, 18–22.
- Burbidge, E. M.; Burbidge, G. R.; Fowler, W. A.; Hoyle, F. *Rev. Mod. Phys.* **1957**, *29*, 547–650.
- Baruah, R.; Duorah, K.; Duorah, H. L. *Astrophys. Space Sci.* **2012**, *340*, 291–305.
- Cowan, J. J.; Thielemann, F. K.; Truran, J. W. *Phys. Rep., Rev. Sect. Phys. Lett.* **1991**, *208*, 267–394.
- Kuroda, P. K. *J. Radioanal. Nucl. Chem.* **1996**, *203*, 591–599.
- Choi, J. S.; Pigford, T. H. *Trans. Am. Nucl. Soc.* **1981**, *39*, 176–177.
- Neuefeind, J.; Soderholm, L.; Skanthakumar, S. *J. Phys. Chem. A* **2004**, *108*, 2733–2739.
- Denning, R. G. *Struct. Bonding (Berlin)* **1992**, *79*, 215–276.
- Denning, R. G. *J. Phys. Chem. A* **2007**, *111*, 4125–4143.
- Christensen, H.; Sunder, S. *Nucl. Technol.* **2000**, *131*, 102–123.
- Sattonnay, G.; Ardois, C.; Corbel, C.; Lucchini, J. F.; Barthe, M. F.; Garrido, F.; Gosset, D. *J. Nucl. Mater.* **2001**, *288*, 11–19.
- Guillaumont, R.; Fanghanel, T.; Volker, N.; Fuger, J.; Palmer, M. R.; Grenthe, I.; Rand, M. H. Update on the Chemical Thermodynamics of Uranium, Neptunium, Plutonium, Americium and Technetium. *Chemical Thermodynamics 5*; Elsevier: Amsterdam, The Netherlands, 2003.
- Dong, W.; Brooks, S. C. *Environ. Sci. Technol.* **2006**, *40*, 4689–4695.
- Berto, S.; Crea, F.; Daniele, P. G.; Gianguzza, A.; Pettignano, A.; Sammartano, S. *Coord. Chem. Rev.* **2012**, *256*, 63–81.
- Soderholm, L.; Skanthakumar, S.; Gorman-Lewis, D.; Jensen, M. P.; Nagy, K. L. *Geochim. Cosmochim. Acta* **2008**, *72*, 140–150.
- Bargar, J. R.; Reitmeyer, R.; Davis, J. A. *Environ. Sci. Technol.* **1999**, *33*, 2481–2484.
- Duff, M. C.; Amrhein, C. *Soil Sci. Soc. Am. J.* **1996**, *60*, 1393–1400.
- Singer, D. M.; Maher, K.; Brown, G. E., Jr. *Geochim. Cosmochim. Acta* **2009**, *73*, 5989–6007.
- Catalano, J. G.; Brown, G. E., Jr. *Geochim. Cosmochim. Acta* **2005**, *69*, 2995–3005.
- Ulrich, K.-U.; Veeramani, H.; Bernier-Latmani, R.; Giammar, D. E. *Geomicrobiol. J.* **2011**, *28*, 396–409.
- Stewart, B. D.; Amos, R. T.; Nico, P. S.; Fendorf, S. *Geomicrobiol. J.* **2011**, *28*, 444–456.
- Stewart, B. D.; Neiss, J.; Fendorf, S. *J. Environ. Qual.* **2007**, *36*, 363–372.
- Singer, D. M.; Chatman, S. M.; Ilton, E. S.; Rosso, K. M.; Banfield, J. F.; Waychunas, G. A. *Environ. Sci. Technol.* **2012**, *46*, 3811–3820.
- Brooks, S. C.; Fredrickson, J. K.; Carroll, S. L.; Kennedy, D. W.; Zachara, J. M.; Plymale, A. E.; Kelly, S. D.; Kemner, K. M.; Fendorf, S. *Environ. Sci. Technol.* **2003**, *37*, 1850–1858.
- Rajan, K. S.; Martell, A. E. *J. Inorg. Nucl. Chem.* **1967**, *29*, 523–529.
- Rajan, K. S.; Martell, A. E. *Inorg. Chem.* **1965**, *4*, 462–469.
- Rajan, K. S.; Martell, A. E. *J. Inorg. Nucl. Chem.* **1964**, *26*, 789–798.
- Rajan, K. S.; Martell, A. E. *J. Inorg. Nucl. Chem.* **1964**, *26*, 1927–1944.
- Crea, F.; De Robertis, A.; De Stefano, C.; Sammartano, S. *Talanta* **2007**, *71*, 948–963.
- Meinrath, G. *J. Radioanal. Nucl. Chem.* **1997**, *224*, 119–126.
- Bernhard, G.; Geipel, G.; Reich, T.; Brendler, V.; Amayri, S.; Nitsche, H. *Radiochim. Acta* **2001**, *89*, 511–518.
- Guenther, A.; Steudtner, R.; Schmeide, K.; Bernhard, G. *Radiochim. Acta* **2011**, *99*, 535–541.
- Pasilis, S. P.; Pemberton, J. E. *Inorg. Chem.* **2003**, *42*, 6793–6800.
- Dodge, C. J.; Francis, A. J. *Radiochim. Acta* **2003**, *91*, 525–532.

- (54) Bailey, E. H.; Mosselmans, J. F. W.; Schofield, P. F. *Chem. Geol.* **2005**, *216*, 1–16.
- (55) Bailey, E. H.; Mosselmans, J. F. W.; Schofield, P. F. *Geochim. Cosmochim. Acta* **2004**, *68*, 1711–1722.
- (56) Hennig, C.; Schmeide, K.; Brendler, V.; Moll, H.; Tsushima, S.; Scheinost, A. C. *Inorg. Chem.* **2007**, *46*, 5882–5892.
- (57) Hennig, C.; Tutschku, J.; Rossberg, A.; Bernhard, G.; Scheinost, A. C. *Inorg. Chem.* **2005**, *44*, 6655–6661.
- (58) Ray, R. S.; Krueger, S.; Roesch, N. *Inorg. Chim. Acta* **2010**, *363*, 263–269.
- (59) Thurman, E. M. *Organic Geochemistry of Natural Waters*; Springer: Dordrecht, The Netherlands, 1985.
- (60) Kharaka, Y. K.; Hanor, J. S. *Deep Fluids in the Continents: I. Sedimentary Basins*; Elsevier: Amsterdam, The Netherlands, 2003; Vol. 5, pp 1–48.
- (61) Jones, D. L. *Plant Soil* **1998**, *205*, 25–44.
- (62) Kantar, C. *Earth-Sci. Rev.* **2007**, *81*, 175–198.
- (63) De Stefano, C.; Gianguzza, A.; Pettignano, A.; Piazzese, D.; Sammartano, S. J. *Radioanal. Nucl. Chem.* **2011**, *289*, 689–697.
- (64) Allen, P. G.; Shuh, D. K.; Bucher, J. J.; Edelstein, N. M.; Reich, T.; Denecke, M. A.; Nitsche, H. *Inorg. Chem.* **1996**, *35*, 784–787.
- (65) Crea, F.; Foti, C.; Sammartano, S. *Talanta* **2008**, *75*, 775–785.
- (66) Pompe, S.; Schmeide, K.; Bubner, M.; Geipel, G.; Heise, K. H.; Bernhard, G.; Nitsche, H. *Radiochim. Acta* **2000**, *88*, 553–558.
- (67) Schild, D.; Marquardt, C. M. *Radiochim. Acta* **2000**, *88*, 587–591.
- (68) Kantar, C.; Honeyman, B. D. J. *Environ. Eng. (Am. Soc. Civ. Eng.)* **2006**, *132*, 247–255.
- (69) Landais, P.; Dubessy, J.; Poty, B.; Robb, L. J. *Org. Geochem.* **1990**, *16*, 601–608.
- (70) Wood, S. A. *Ore Geol. Rev.* **1996**, *11*, 1–31.
- (71) Crancon, P.; van der Lee, J. *Radiochim. Acta* **2003**, *91*, 673–679.
- (72) Zhou, P.; Gu, B. H. *Environ. Sci. Technol.* **2005**, *39*, 4435–4440.
- (73) Bencheikh-Latmani, R.; Leckie, J. O. *Geochim. Cosmochim. Acta* **2003**, *67*, 4057–4066.
- (74) Matsunaga, T.; Nagao, S.; Ueno, T.; Takeda, S.; Amano, H.; Tkachenko, Y. *Appl. Geochem.* **2004**, *19*, 1581–1599.
- (75) Choppin, G. R. *Radiochim. Acta* **1992**, *58–9*, 113–120.
- (76) Zeh, P.; Kim, J. I.; Marquardt, C. M.; Artinger, R. *Radiochim. Acta* **1999**, *87*, 23–28.
- (77) Andre, C.; Choppin, G. R. *Radiochim. Acta* **2000**, *88*, 613–616.
- (78) Kaszuba, J. P.; Runde, W. H. *Environ. Sci. Technol.* **1999**, *33*, 4427–4433.
- (79) Felmy, A. R.; Cantrell, K. J.; Conradson, S. D. *Phys. Chem. Earth* **2010**, *35*, 292–297.
- (80) Zavarin, M.; Powell, B. A.; Bourbin, M.; Zhao, P.; Kersting, A. B. *Environ. Sci. Technol.* **2012**, *46*, 2692–2698.
- (81) Keeney-Kennicutt, W. L.; Morse, J. W. *Geochim. Cosmochim. Acta* **1985**, *49*, 2577–2588.
- (82) Powell, B. A.; Fjeld, R. A.; Kaplan, D. I.; Coates, J. T.; Serkiz, S. M. *Environ. Sci. Technol.* **2005**, *39*, 2107–2114.
- (83) Powell, B. A.; Fjeld, R. A.; Kaplan, D. I.; Coates, J. T.; Serkiz, S. M. *Environ. Sci. Technol.* **2004**, *38*, 6016–6024.
- (84) Soderholm, L.; Almond, P. M.; Skanthakumar, S.; Wilson, R. E.; Burns, P. C. *Angew. Chem., Int. Ed.* **2008**, *47*, 298–302.
- (85) Schmeide, K.; Reich, T.; Sachs, S.; Bernhard, G. *Inorg. Chim. Acta* **2006**, *359*, 237–242.
- (86) Rai, D.; Serne, R. J.; Moore, D. A. *Soil Sci. Soc. Am. J.* **1980**, *44*, 490–495.
- (87) Qafoku, N. P.; Icenhower, J. P. *Rev. Environ. Sci. Bio/Technol.* **2008**, *7*, 355–380.
- (88) Geckeis, H.; Rabung, T. J. *Contam. Hydrol.* **2008**, *102*, 187–195.
- (89) Stumm, W. *Chemistry of the Solid–Water Interface: Processes at the Mineral–Water and Particle–Water Interfaces in Natural Systems*; Wiley Interscience: New York, 1992.
- (90) Brown, G. E., Jr.; Henrich, V. E.; Casey, W. H.; Clark, D. L.; Eggleston, C.; Felmy, A.; Goodman, D. W.; Grätzel, M.; Maciel, G.; McCarthy, M. I.; Neelson, K.; Sverjensky, D. A.; Toney, M. F.; Zachara, J. M. *Chem. Rev.* **1999**, *99*, 77–174.
- (91) Catalano, J. G.; Park, C.; Fenter, P.; Zhang, Z. *Geochim. Cosmochim. Acta* **2008**, *72*.
- (92) Towle, S. N.; Bargar, J. R.; Brown, G. E., Jr.; Parks, G. A. J. *Colloid Interface Sci.* **1997**, *187*, 62–82.
- (93) Catalano, J. G.; Heald, S. M.; Zachara, J. M.; Brown, G. E., Jr. *Environ. Sci. Technol.* **2004**, *38*, 2822–2828.
- (94) Singer, D. M.; Zachara, J. M.; Brown, G. E., Jr. *Environ. Sci. Technol.* **2009**, *43*, 630–636.
- (95) Kohler, M.; Wieland, E.; Leckie, J. O. Metal–ligand–surface interactions during sorption of uranyl and neptunyl on oxides and silicates. In *Proceedings of the 7th International Symposium on Water–Rock Interaction*; Kharaka, Y. K., Maest, A. S., Eds.; A. A. Balkema: Rotterdam, The Netherlands, 1992; Vol. 1, pp 51–54.
- (96) Sverjensky, D. A. *Geochim. Cosmochim. Acta* **1994**, *58*, 3123–3129.
- (97) Hingston, F. J.; Quirk, J. P.; Posner, A. M. J. *Soil Sci.* **1972**, *23*, 177–192.
- (98) Parks, G. A. *Adv. Chem. Ser.* **1967**, *121*–160.
- (99) Schroth, B. K.; Sposito, G. *Clays Clay Miner.* **1997**, *45*, 85–91.
- (100) Combes, J. M.; Chisholm-Brause, C. J.; Brown, G. E., Jr.; Parks, G. A.; Conradson, S. D.; Eller, P. G.; Triay, I. R.; Hobart, D. E.; Meijer, A. *Environ. Sci. Technol.* **1992**, *26*, 376–382.
- (101) James, R. O.; Healy, T. W. J. *Colloid Interface Sci.* **1972**, *40*, 53–64.
- (102) Duff, M. C.; Hunter, D. B.; Triay, I. R.; Bertsch, P. M.; Sutton, S. R.; Shea-Mccarthy, G.; Kitten, J.; Chipera, S. J.; Vaniman, D. T. *Environ. Sci. Technol.* **1999**, *33*, 2163–2169.
- (103) Thompson, H. A.; Brown, G. E.; Parks, G. A. *Am. Mineral.* **1997**, *82*, 483–496.
- (104) Sekine, K. P.; Payne, T. E.; Waite, T. D.; Davis, J. A. *International alligator rivers analogue project (18): Experimental study of uranium adsorption on kaolinite—pH dependence in air-equilibrated system*; JAERI Memo 03-036; Japan Atomic Energy Research Institute: Tokyo, 1991.
- (105) Thompson, H. A.; Parks, G. A.; Brown, G. E., Jr. Structure and composition of uranium(VI) sorption complexes at the kaolinite–water interface. In *Adsorption of Metals by Geomedia, Variables, Mechanisms, and Model Applications*; Jenne, E. A., Ed.; Academic Press: New York, 1998; pp 349–370.
- (106) Chisholm-Brause, C. J.; Conradson, S. D.; Buscher, C. T.; Eller, P. G.; Morris, D. E. *Geochim. Cosmochim. Acta* **1994**, *58*, 3625–3631.
- (107) Bargar, J. R.; Reitmeyer, R.; Lenhart, J. J.; Davis, J. A. *Geochim. Cosmochim. Acta* **2000**, *64*, 2737–2749.
- (108) Dong, W. M.; Ball, W. P.; Liu, C. X.; Wang, Z. M.; Stone, A. T.; Bai, J.; Zachara, J. M. *Environ. Sci. Technol.* **2005**, *39*, 7949–7955.
- (109) Fox, P. M.; Davis, J. A.; Zachara, J. M. *Geochim. Cosmochim. Acta* **2006**, *70*, 1379–1387.
- (110) Brown, G. E., Jr.; Sturchio, N. C. *Rev. Mineral. Geochem.* **2002**, *49*, 1–115.
- (111) Antonio, M. R.; Soderholm, L. X-ray absorption spectroscopy of the actinides. In *The Chemistry of the Actinide and Transactinide Elements*, 4th ed.; Morss, L. R., Edelstein, N. M., Fuger, J., Eds.; Springer: Dordrecht, The Netherlands, 2010; pp 3475–3593.
- (112) Tan, X.; Fang, M.; Wang, X. *Molecules* **2010**, *15*, 8431–8468.
- (113) Greathouse, J. A.; Stellalevinsohn, H. R.; Denecke, M. A.; Bauer, A.; Pabalan, R. T. *Clays Clay Miner.* **2005**, *53*, 278–286.
- (114) Schlegel, M. L.; Descostes, M. *Environ. Sci. Technol.* **2009**, *43*, 8593–8598.
- (115) Stumpf, T.; Hennig, C.; Bauer, A.; Denecke, M. A.; Fanghanel, T. *Radiochim. Acta* **2004**, *92*, 133–138.
- (116) Krepelova, A.; Reich, T.; Sachs, S.; Drebert, J.; Bernhard, G. J. *Colloid Interface Sci.* **2008**, *319*, 40–47.
- (117) Chardon, E. S.; Bosbach, D.; Bryan, N. D.; Lyon, I. C.; Marquardt, C.; Roemer, J.; Schild, D.; Vaughan, D. J.; Wincott, P. L.; Wogelius, R. A.; Livens, F. R. *Geochim. Cosmochim. Acta* **2008**, *72*, 288–297.
- (118) Walter, M.; Arnold, T.; Reich, T.; Bernhard, G. *Environ. Sci. Technol.* **2003**, *37*, 2898–2904.

- (119) Zeng, H.; Giammar, D. E. *J. Nanopart. Res.* **2011**, *13*, 3741–3754.
- (120) Zeng, H.; Singh, A.; Basak, S.; Ulrich, K.-U.; Sahu, M.; Biswas, P.; Catalano, J. G.; Giammar, D. E. *Environ. Sci. Technol.* **2009**, *43*, 1373–1378.
- (121) Tang, Y.; McDonald, J.; Reeder, R. J. *Environ. Sci. Technol.* **2009**, *43*, 4452–4458.
- (122) Tang, Y.; Reeder, R. J. *Geochim. Cosmochim. Acta* **2009**, *73*, 2727–2743.
- (123) Elzinga, E. J.; Tait, C. D.; Reeder, R. J.; Rector, K. D.; Donohoe, R. J.; Morris, D. E. *Geochim. Cosmochim. Acta* **2004**, *68*, 2437–2448.
- (124) Reeder, R. J.; Elzinga, E. J.; Tait, C. D.; Rector, K. D.; Donohoe, R. J.; Morris, D. E. *Geochim. Cosmochim. Acta* **2004**, *68*, 4799–4808.
- (125) Webb, S. M.; Fuller, C. C.; Tebo, B. M.; Bargar, J. R. *Environ. Sci. Technol.* **2006**, *40*, 771–777.
- (126) Teterin, A. Y.; Maslakov, K. I.; Teterin, Y. A.; Kalmykov, S. N.; Ivanov, K. E.; Vukcevic, L.; Khasanova, A. B.; Shcherbina, N. S. *Russ. J. Inorg. Chem.* **2006**, *51*, 1937–1944.
- (127) Heberling, F.; Brendebach, B.; Bosbach, D. *J. Contam. Hydrol.* **2008**, *102*, 246–252.
- (128) Wilk, P. A.; Shaughnessy, D. A.; Wilson, R. E.; Nitsche, H. *Environ. Sci. Technol.* **2005**, *39*, 2608–2615.
- (129) Stumpf, S.; Stumpf, T.; Dardenne, K.; Hennig, C.; Foerstendorf, H.; Klenze, R.; Fanghanel, T. *Environ. Sci. Technol.* **2006**, *40*, 3522–3528.
- (130) Kalmykov, S. N.; Kriventsov, V. V.; Teterin, Y. A.; Novikov, A. P. *C. R. Chim.* **2007**, *10*, 1060–1066.
- (131) Mueller, K.; Foerstendorf, H.; Brendler, V.; Bernhard, G. *Environ. Sci. Technol.* **2009**, *43*, 7665–7670.
- (132) Nico, P. S.; Stewart, B. D.; Fendorf, S. *Environ. Sci. Technol.* **2009**, *43*, 7391–7396.
- (133) Stubbs, J. E.; Elbert, D. C.; Veblen, D. R.; Zhu, C. *Environ. Sci. Technol.* **2006**, *40*, 2108–2113.
- (134) Michel, F. M.; Barron, V.; Torrent, J.; Morales, M. P.; Serna, C. J.; Boily, J.-F.; Liu, Q.; Ambrosini, A.; Cismasu, A. C.; Brown, G. E., Jr. *Proc. Natl. Acad. Sci. U.S.A.* **2010**, *107*, 2787–2792.
- (135) Michel, F. M.; Ehm, L.; Antao, S. M.; Lee, P. L.; Chupas, P. J.; Liu, G.; Strongin, D. R.; Schoonen, M. A. A.; Phillips, B. L.; Parise, J. B. *Science* **2007**, *316*, 1726–1729.
- (136) Cornell, R. M.; Schwertmann, U. *The Iron Oxides: Structure, Properties, Reactions, Occurrence and Uses*; Wiley-VHC GmbH & Co. KGaA Publishers: New York, 2003.
- (137) Shannon, R. D. *Acta Crystallogr., Sect. A* **1976**, *32*, 751–767.
- (138) Blundy, J.; Wood, B. *Earth Planet. Sci. Lett.* **2003**, *210*, 383–397.
- (139) Ildefonse, P.; Kirkpatrick, R. J.; Montez, B.; Calas, G.; Flank, A. M.; Lagarde, P. *Clays Clay Miner.* **1994**, *42*, 276–287.
- (140) Cismasu, A. C.; Michel, F. M.; Tcaciuc, A. P.; Tyliczszak, T.; Brown, G. E., Jr. *C. R. Geosci.* **2011**, *343*, 210–218.
- (141) Combes, J. M.; Manceau, A.; Calas, G.; Bottero, J. Y. *Geochim. Cosmochim. Acta* **1989**, *53*, 583–594.
- (142) Maher, K.; Bethke, C. M.; Massey, M. S. Fall Meeting of American Geophysical Union, 2011; Abstract V22B-05.
- (143) Farges, F.; Benzerara, K.; Brown, G. E., Jr. *Am. Inst. Phys. Conf. Proc.* **2007**, *882*, 223–225.
- (144) Choppin, G. R.; Wong, P. J. *Aquat. Geochem.* **1998**, *4*, 77–101.
- (145) Myneni, S. C. B.; Brown, J. T.; Martinez, G. A.; Meyer-Ilse, W. *Science* **1999**, *286*, 1335–1337.
- (146) Sutton, R.; Sposito, G. *Environ. Sci. Technol.* **2005**, *39*, 9009–9015.
- (147) Baldock, J. A.; Oades, J. M.; Waters, A. G.; Peng, X.; Vassallo, A. M.; Wilson, M. A. *Biogeochemistry* **1992**, *16*, 1–42.
- (148) Monsallier, J.-M.; Artinger, R.; Denecke, M. A.; Scherbaum, F. J.; Buckau, G.; Kim, J.-I. *Radiochim. Acta* **2003**, *91*, 567–574.
- (149) Lovley, D. R.; Phillips, E. J. P.; Gorby, Y. A.; Landa, E. R. *Nature* **1991**, *350*, 413–416.
- (150) Neu, M. P.; Ruggiero, C. E.; Francis, A. J. Bioinorganic chemistry of plutonium and interactions of plutonium with microorganisms and plants. In *Advances in Plutonium Chemistry 1967–2000*; Hoffman, D., Ed.; American Nuclear Society: LaGrange Park, IL, 2002; pp 169–211.
- (151) Lloyd, J. R. *FEMS Microbiol. Rev.* **2003**, *27*, 411–425.
- (152) Fein, J. B.; Daughney, C. J.; Yee, N.; Davis, T. A. *Geochim. Cosmochim. Acta* **1997**, *61*, 3319–3328.
- (153) Guine, V.; Spadini, L.; Sarret, G.; Muris, M.; Delolme, C.; Gaudet, J. P.; Martins, J. M. F. *Environ. Sci. Technol.* **2006**, *40*, 1806–1813.
- (154) Ha, J.; Gelibert, A.; Spormann, A. M.; Brown, G. E., Jr. *Geochim. Cosmochim. Acta* **2010**, *74*, 1–15.
- (155) Jiang, W.; Saxena, A.; Song, B.; Ward, B. B.; Beveridge, T. J.; Myneni, S. C. B. *Langmuir* **2004**, *20*, 11433–11442.
- (156) Kelly, S. D.; Boyanov, M. I.; Bunker, B. A.; Fein, J. B.; Fowle, D. A.; Yee, N.; Kemner, K. M. *J. Synchrotron Radiat.* **2001**, *8*, 946–948.
- (157) Kelly, S. D.; Kemner, K. M.; Fein, J. B.; Fowle, D. A.; Boyanov, M. I.; Bunker, B. A.; Yee, N. *Geochim. Cosmochim. Acta* **2002**, *66*, 3855–3871.
- (158) Sarret, G.; Manceau, A.; Spadini, L.; Roux, J. C.; Hazemann, J. L.; Soldo, Y.; Eybert-Berard, L.; Menthonnex, J. J. *Environ. Sci. Technol.* **1998**, *32*, 1648–1655.
- (159) Yee, N.; Fowle, D. A.; Ferris, F. G. *Geochim. Cosmochim. Acta* **2004**, *68*, 3657–3664.
- (160) Lloyd, J. R.; Yong, P.; Macaskie, L. E. *Environ. Sci. Technol.* **2000**, *34*, 1297–1301.
- (161) Campbell, K. M.; Kukkadapu, R. K.; Qafoku, N. P.; Peacock, A. D.; Leshner, E.; Williams, K. H.; Bargar, J. R.; Wilkins, M. J.; Figueroa, L.; Ranville, J.; Davis, J. A.; Long, P. E. *Appl. Geochem.* **2012**, *27*, 1499–1511.
- (162) Sharp, J. O.; Lezama-Pacheco, J. S.; Schofield, E. J.; Junier, P.; Ulrich, K.-U.; Chinni, S.; Veeramani, H.; Margot-Roquier, C.; Webb, S. M.; Tebo, B. M.; Giammar, D. E.; Bargar, J. R.; Bernier-Latmani, R. *Geochim. Cosmochim. Acta* **2011**, *75*, 6497–6510.
- (163) Fredrickson, J. K.; Zachara, J. M.; Kennedy, D. W.; Duff, M. C.; Gorby, Y. A.; Li, S. M. W.; Krupka, K. M. *Geochim. Cosmochim. Acta* **2000**, *64*, 3085–3098.
- (164) Fowle, D. A.; Fein, J. B.; Martin, A. M. *Environ. Sci. Technol.* **2000**, *34*, 3737–3741.
- (165) Haas, J. R.; Dichristina, T. J.; Wade, R. *Chem. Geol.* **2001**, *180*, 33–54.
- (166) Panak, P. J.; Kim, M. A.; Klenze, R.; Kim, J. I.; Fanghanel, T. *Radiochim. Acta* **2005**, *93*, 133–139.
- (167) Hennig, C.; Panak, P. J.; Reich, T.; Rossberg, A.; Raff, J.; Selenska-Pobell, S.; Matz, W.; Bucher, J. J.; Bernhard, G.; Nitsche, H. *Radiochim. Acta* **2001**, *89*, 625–631.
- (168) Hunter, R. J. *Introduction to Modern Colloid Science*; Oxford University Press: Oxford, U.K., 1993.
- (169) McCarthy, J. F.; Zachara, J. M. *Environ. Sci. Technol.* **1989**, *23*, 496–502.
- (170) Grolimund, D.; Borkovec, M. *Environ. Sci. Technol.* **2005**, *39*, 6378–6386.
- (171) Grolimund, D.; Borkovec, M.; Barmettler, K.; Sticher, H. *Environ. Sci. Technol.* **1996**, *30*, 3118–3123.
- (172) Buffle, J.; Wilkinson, K. J.; Stoll, S.; Filella, M.; Zhang, J. W. *Environ. Sci. Technol.* **1998**, *32*, 2887–2899.
- (173) Buddemeier, R. W.; Hunt, J. R. *Appl. Geochem.* **1988**, *3*, 535–548.
- (174) Kraus, K. A.; Nelson, F. J. *Am. Chem. Soc.* **1950**, *72*, 3901–3906.
- (175) Neck, V.; Altmaier, M.; Fanghaenel, T. C. R. *Chim.* **2007**, *10*, 959–977.
- (176) Neck, V.; Kim, J. I. *Radiochim. Acta* **2001**, *89*, 1–16.
- (177) Neu, M. P.; Schulze, R. K.; Conradson, S. D.; Farr, J. D.; Haire, R. G. *Polymeric plutonium(IV) hydroxide: Formation, prevalence, and structural and physical characteristics*; Los Alamos National Laboratory: Los Alamos, NM, 1997.
- (178) Conradson, S. D. *Appl. Spectrosc.* **1998**, *52*, 252A–279A.

- (179) Altmaier, M.; Neck, V.; Fanghanel, T. *Radiochim. Acta* **2004**, *92*, 537–543.
- (180) Singer, D. M.; Farges, F.; Brown, G. E., Jr. *Geochim. Cosmochim. Acta* **2009**, *73*, 3593–3611.
- (181) Sullivan, J. C.; Zielen, A. J.; Hindman, J. C. *J. Am. Chem. Soc.* **1961**, *83*, 3373–3378.
- (182) Burns, P. C.; Kubatko, K. A.; Sigmon, G.; Fryer, B. J.; Gagnon, J. E.; Antonio, M. R.; Soderholm, L. *Angew. Chem., Int. Ed.* **2005**, *44*, 2135–2139.
- (183) Sigmon, G. E.; Weaver, B.; Kubatko, K.-A.; Burns, P. C. *Inorg. Chem.* **2009**, *48*, 10907–10909.
- (184) Sigmon, G. E.; Ling, J.; Unruh, D. K.; Moore-Shay, L.; Ward, M.; Weaver, B.; Burns, P. C. *J. Am. Chem. Soc.* **2009**, *131*, 16648–16649.
- (185) Sigmon, G. E.; Unruh, D. K.; Ling, J.; Weaver, B.; Ward, M.; Pressprich, L.; Simonetti, A.; Burns, P. C. *Angew. Chem., Int. Ed.* **2009**, *48*, 2737–2740.
- (186) Krivovichev, S. V.; Kahlenberg, V.; Tananaev, I. G.; Kaindil, R.; Mersdorf, E.; Myasoedov, B. F. *J. Am. Chem. Soc.* **2005**, *127*, 1072–1073.
- (187) Burns, P. C.; Ikeda, Y.; Czerwinski, K. *MRS Bull.* **2010**, *35*, 868–876.
- (188) Forbes, T. Z.; Horan, P.; Devine, T.; McInnis, D.; Burns, P. C. *Am. Mineral.* **2011**, *96*, 202–206.
- (189) Schmidt, M.; Wilson, R. E.; Lee, S. S.; Soderholm, L.; Fenter, P. *Langmuir* **2012**, *28*, 2620–2627.
- (190) Hsi, C. K. D.; Langmuir, D. *Geochim. Cosmochim. Acta* **1985**, *49*, 1931–1941.
- (191) Waite, T. D.; Davis, J. A.; Payne, T. E.; Waychunas, G. A.; Xu, N. *Geochim. Cosmochim. Acta* **1994**, *58*, 5465–5478.
- (192) Langmuir, D. *Geochim. Cosmochim. Acta* **1978**, *42*, 547–569.
- (193) Ames, L. L.; McGarrah, J. E.; Walker, B. A. *Clays Clay Miner.* **1983**, *31*, 321–334.
- (194) Moulin, V.; Moulin, C. *Radiochim. Acta* **2001**, *89*, 773–778.
- (195) Nagasaki, S.; Tanaka, S.; Suzuki, A. *J. Nucl. Mater.* **1997**, *244*, 29–35.
- (196) Novikov, A. P.; Kalmykov, S. N.; Utsunomiya, S.; Ewing, R. C.; Horreard, F.; Merkulov, A.; Clark, S. B.; Tkachev, V. V.; Myasoedov, B. F. *Science* **2006**, *314*, 638–641.
- (197) Shcherbina, N. S.; Perminova, I. V.; Kalmykov, S. N.; Kovalenko, A. N.; Haire, R. G.; Novikov, A. P. *Environ. Sci. Technol.* **2007**, *41*, 7010–7015.
- (198) Kersting, A. B.; Efurud, D. W.; Finnegan, D. L.; Rokop, D. J.; Smith, D. K.; Thompson, J. L. *Nature* **1999**, *397*, 56–59.
- (199) Kaplan, D. I.; Bertsch, P. M.; Adriano, D. C.; Orlandini, K. A. *Radiochim. Acta* **1994**, *66–7*, 181–187.
- (200) Kaplan, D. J.; Hunter, D. B.; Bertsch, P. M.; Bajt, S.; Adriano, D. D. *Environ. Sci. Technol.* **1994**, *28*, 1186–1189.
- (201) Burns, P. C.; Ewing, R. C.; Navrotsky, A. *Science* **2012**, *335*, 1184–1188.
- (202) Farnan, I.; Cho, H.; Weber, W. J. *Nature* **2007**, *445*, 190–193.
- (203) Kubatko, K. A. H.; Helean, K. B.; Navrotsky, A.; Burns, P. C. *Science* **2003**, *302*, 1191–1193.
- (204) Weber, W. J.; Ewing, R. C.; Catlow, C. R. A.; de la Rubia, T. D.; Hobbs, L. W.; Kinoshita, C.; Matzke, H.; Motta, A. T.; Nastasi, M.; Salje, E. K. H.; Vance, E. R.; Zinkle, S. J. *J. Mater. Res.* **1998**, *13*, 1434–1484.
- (205) Finch, R. J.; Ewing, R. C. *J. Nucl. Mater.* **1992**, *190*, 133–156.
- (206) Finch, R. J.; Miller, M. L.; Ewing, R. C. *Radiochim. Acta* **1992**, *58–9*, 433–443.
- (207) Percy, E. C.; Prikryl, J. D.; Murphy, W. M.; Leslie, B. W. *Appl. Geochem.* **1994**, *9*, 713–732.
- (208) Finch, R.; Murakami, T. *Rev. Mineral.* **1999**, *38*, 91–179.
- (209) Murakami, T.; Ohnuki, T.; Isobe, H.; Sato, T. *Am. Mineral.* **1997**, *82*, 888–899.
- (210) Murakami, T.; Sato, T.; Ohnuki, T.; Isobe, H. *Chem. Geol.* **2005**, *221*, 117–126.
- (211) Burns, P. C.; Klingensmith, A. L. *Elements* **2006**, *2*, 351–356.
- (212) Burns, P. C.; Miller, M. L.; Ewing, R. C. *Can. Mineral.* **1996**, *34*, 845–880.
- (213) Isobe, H.; Murakami, T.; Ewing, R. C. *J. Nucl. Mater.* **1992**, *190*, 174–187.
- (214) McKinley, J. P.; Zachara, J. M.; Liu, C. X.; Heald, S. C.; Prenitzer, B. L.; Kempshall, B. W. *Geochim. Cosmochim. Acta* **2006**, *70*, 1873–1887.
- (215) Wang, Z.; Zachara, J. M.; McKinley, J. P.; Smith, S. C.; Resch, C. T.; Qafoku, O. S. *Abstr. Pap. Am. Chem. Soc.* **2004**, *228*, U702–U703.
- (216) Phillips, D. H.; Watson, D. B.; Roh, Y. *Environ. Sci. Technol.* **2007**, *41*, 7653–7660.
- (217) Wang, Z. M.; Zachara, J. M.; Gassman, P. L.; Liu, C. X.; Qafoku, O.; Yantasee, W.; Catalano, J. G. *Geochim. Cosmochim. Acta* **2005**, *69*, 1391–1403.
- (218) Klingensmith, A. L.; Burns, P. C. *Am. Mineral.* **2007**, *92*, 1946–1951.
- (219) Klingensmith, A. L.; Deely, K. M.; Kinman, W. S.; Kelly, V.; Burns, P. C. *Am. Mineral.* **2007**, *92*, 662–669.
- (220) Zachara, J. M.; Serne, J.; Freshley, M.; Mann, F.; Anderson, F.; Wood, M.; Jones, T.; Myers, D. *Vadose Zone J.* **2007**, *6*, 985–1003.
- (221) McKinley, J. P.; Zachara, J. M.; Wan, J.; McCready, D. E.; Heald, S. M. *Vadose Zone J.* **2007**, *6*, 1004–1017.
- (222) Fredrickson, J. K.; Brockman, F. J.; Bjornstad, B. N.; Long, P. E.; Li, S. W.; McKinley, J. P.; Wright, J. V.; Conca, J. L.; Kieft, T. L.; Balkwill, D. L. *Geomicrobiol. J.* **1993**, *11*, 95–107.
- (223) Maher, K.; DePaolo, D. J.; Conrad, M. E.; Serne, R. J. *Water Resour. Res.* **2003**, *39*, 1029–1043.
- (224) DePaolo, D. J.; Conrad, M. E.; Maher, K.; Gee, G. W. *Vadose Zone J.* **2004**, *3*, 220–232.
- (225) Singleton, M. J.; Maher, K.; DePaolo, D. J.; Conrad, M. E.; Dresel, P. E. *J. Hydrol.* **2006**, *321*, 39–58.
- (226) Peterson, R. E.; Freeman, E. J.; Murray, C. J.; Thorne, P. D.; Truex, M. J.; Vermuel, V. R.; Williams, M. D.; Yabusaki, S. B.; Zachara, J. M.; Lindberg, J. L.; McDonald, J. P. *Contaminants of potential concern in the 300-ff-5 operable unit: Expanded annual groundwater report for fiscal year 2004*; Pacific Northwest National Laboratory: Richland, WA, 2005; PNNL-15127.
- (227) Zachara, J. M.; Davis, J. A.; McKinley, J. P.; Wellman, D. M.; Liu, C.; Qafoku, N. P.; Yabusaki, S. *Uranium geochemistry in vadose zone and aquifer sediments from the 300 area uranium plume*; Pacific Northwest National Laboratory: Richland, WA, 2005; PNNL-15121.
- (228) Reich, T.; Moll, H.; Denecke, M. A.; Geipel, G.; Bernhard, G.; Nitsche, H. *Radiochim. Acta* **1996**, *74*, 219–223.
- (229) Neiss, J.; Stewart, B. D.; Nico, P. S.; Fendorf, S. *Environ. Sci. Technol.* **2007**, *41*, 7343–7348.
- (230) Stewart, B. D.; Amos, R. T.; Fendorf, S. *J. Environ. Qual.* **2011**, *40*, 90–97.
- (231) Zheng, Z. P.; Tokunaga, T. K.; Wan, J. M. *Environ. Sci. Technol.* **2003**, *37*, 5603–5608.
- (232) Stewart, B. D.; Mayes, M. A.; Fendorf, S. *Environ. Sci. Technol.* **2010**, *44*, 928–934.
- (233) Wan, J. M.; Tokunaga, T. K.; Brodie, E.; Wang, Z. M.; Zheng, Z. P.; Herman, D.; Hazen, T. C.; Firestone, M. K.; Sutton, S. R. *Environ. Sci. Technol.* **2005**, *39*, 6162–6169.
- (234) Ilton, E. S.; Qafoku, N. P.; Liu, C.; Moore, D. A.; Zachara, J. M. *Environ. Sci. Technol.* **2008**, *42*, 1565–1561.
- (235) Maher, K.; DePaolo, D. J.; Christensen, J. N. *Geochim. Cosmochim. Acta* **2006**, *70*, 4417–4435.
- (236) Wan, J.; Tokunaga, T. K.; Kim, Y.; Wang, Z. M.; Lanzirotti, A.; Saiz, E.; Serne, R. J. *Environ. Sci. Technol.* **2008**, *42*, 1973–1978.
- (237) Gephart, R. E.; Lundgren, R. E. *Hanford tank clean up: A guide to understanding the technical issues*; Pacific Northwest Laboratory: Richland, WA, 1996; PNL-10773.
- (238) U.S. DOE. *Vadose zone characterization project at the Hanford tank farms-SX Tank Farm*; U.S. Department of Energy: Grand Junction, CO, 1996; DOE/ID/12584-268.

- (239) Hanlon, B. M. *Waste tank summary report for month ending July 31, 2000*; CH2M Hill Hanford Group, Inc.: Richland, WA, 2000; HN-EP-0182-148;
- (240) Jones, T. E.; Wood, M. I.; Corbin, R. A.; Simpson, B. C. *Preliminary inventory estimates for single-shell tank leaks in B, BX, and BY Tank Farms*; CH2M Hill Hanford Group, Inc.: Richland, WA, 2001; RPP-7389.
- (241) Christensen, J. N.; Dresel, P. E.; Conrad, M. E.; Maher, K.; Depaolo, D. J. *Environ. Sci. Technol.* **2004**, *38*, 3330–3337.
- (242) Liu, C. X.; Zachara, J. M.; Qafoku, O.; McKinley, J. P.; Heald, S. M.; Wang, Z. M. *Geochim. Cosmochim. Acta* **2004**, *68*, 4519–4537.
- (243) Liu, C. X.; Zachara, J. M.; Yantasee, W.; Majors, P. D.; McKinley, J. P. *Water Resour. Res.* **2006**, *42*, W12420(1–15).
- (244) Wang, Z. M.; Zachara, J. M.; Yantasee, W.; Gassman, P. L.; Liu, C. X.; Joly, A. G. *Environ. Sci. Technol.* **2004**, *38*, 5591–5597.
- (245) Ilton, E. S.; Liu, C. X.; Yantasee, W.; Wang, Z. M.; Moore, D. A.; Felmy, A. R.; Zachara, J. M. *Geochim. Cosmochim. Acta* **2006**, *70*, 4836–4849.
- (246) Kerisit, S.; Liu, C. *Environ. Sci. Technol.* **2012**, *46*, 1632–1640.
- (247) Wan, J.; Kim, Y.; Tokunaga, T. K.; Wang, Z.; Dixit, S.; Steefel, C. I.; Saiz, E.; Kunz, M.; Tamura, N. *Environ. Sci. Technol.* **2009**, *43*, 2247–2253.
- (248) Williams, B. A.; Brown, C. F.; Um, W.; Nimmons, M. J.; Peterson, R. E.; Bjornstad, B. N.; Lanigan, D. C.; Serne, R. J.; Spane, F. A.; Rockhold, M. L. *Limited field investigation report for uranium contamination in the 300 Area, 300-FF-5 operable unit, Hanford Site, Washington*; Pacific Northwest National Laboratory: Richland, WA, 2007; PNNL-16435.
- (249) Catalano, J. G.; McKinley, J. P.; Zachara, J. M.; Heald, S. M.; Smith, S. C.; Brown, G. E., Jr. *Environ. Sci. Technol.* **2006**, *40*, 2517–2524.
- (250) Peng, S.; Hu, Q.; Ewing, R. P.; Liu, C.; Zachara, J. M. *Environ. Sci. Technol.* **2012**, *46*, 2025–2032.
- (251) Katsenovich, Y. P.; Carvajal, D. A.; Wellman, D. M.; Lagos, L. E. *Chem. Geol.* **2012**, *308*, 1–9.
- (252) Arai, Y.; Marcus, M. K.; Tamura, N.; Davis, J. A.; Zachara, J. M. *Environ. Sci. Technol.* **2007**, *41*, 4633–4639.
- (253) Lichtner, P. C.; Hammond, G. E. *Vadose Zone J.* **2012**, *11*.
- (254) Hay, M. B.; Stoliker, D. L.; Davis, J. A.; Zachara, J. M. *Water Resour. Res.* **2011**, *47*.
- (255) U.S. DOE. *Final observational work plan for the UMTRA project Old Rifle Site, August 1999. GJO-99-88-tar. Rev. 1*; U.S. Department of Energy: Grand Junction, CO, 1999.
- (256) Williams, K. H.; Long, P. E.; Davis, J. A.; Wilkins, M. J.; N'Guessan, A. L.; Steefel, C. I.; Yang, L.; Newcomer, D.; Spane, F. A.; Kerkhof, L. J.; McGuinness, L.; Dayvault, R.; Lovley, D. R. *Geomicrobiol. J.* **2011**, *28*, 519–539.
- (257) U.S. DOE. *Ground Water Compliance Action Plan for the Old Rifle, Colorado, UMTRA Project Site, GJO-2000-177-TA*; U.S. Department of Energy: Grand Junction, CO, 2001; p 21.
- (258) U.S. DOE. *Remedial Action Plan and Site Conceptual Design for Stabilization of the Inactive Uranium Mill Tailings Sites at Rifle, CO. DOE/UMTRA-050506-0000-vol.2. DE93 010763*; U.S. Department of Energy: Grand Junction, CO, 1992.
- (259) Anderson, R. T.; Vrionis, H. A.; Ortiz-Bernad, I.; Resch, C. T.; Long, P. E.; Dayvault, R.; Karp, K.; Marutzky, S.; Metzler, D. R.; Peacock, A.; White, D. C.; Lowe, M.; Lovley, D. R. *Appl. Environ. Microbiol.* **2003**, *69*, 5884–5891.
- (260) Yabusaki, S. B.; Fang, Y.; Long, P. E.; Resch, C. T.; Peacock, A. D.; Komlos, J.; Jaffe, P. R.; Morrison, S. J.; Dayvault, R. D.; White, D. C.; Anderson, R. T. *J. Contam. Hydrol.* **2007**, *93*, 216–235.
- (261) Hyun, S. P.; Fox, P. M.; Davis, J. A.; Campbell, K. M.; Hayes, K. F.; Long, P. E. *Environ. Sci. Technol.* **2009**, *43*, 9368–9373.
- (262) Cerrato, J. M.; Barrows, C. J.; Blue, L. Y.; Lezama-Pacheco, J. S.; Bargar, J. R.; Giammar, D. E. *Environ. Sci. Technol.* **2012**, *46*, 2731–2737.
- (263) Robinson, P. *Uranium Mill Tailings Remediation Performed by the U.S. DOE: An Overview*; Southwest Research and Information Center: Albuquerque, NM, 2004.
- (264) Vrionis, H. A.; Anderson, R. T.; Ortiz-Bernad, I.; O'Neill, K. R.; Resch, C. T.; Peacock, A. D.; Dayvault, R.; White, D. C.; Long, P. E.; Lovley, D. R. *Appl. Environ. Microbiol.* **2005**, *71*, 6308–6318.
- (265) Wrighton, K. C.; Thomas, B. C.; Sharon, I.; Miller, C. S.; Castelle, C.; VerBerkmoes, N. C.; Wilkins, M. J.; Hettich, R. L.; Lipton, M. L.; Williams, K. H.; Long, P. E.; Banfield, J. F. *Science* **2012**, *337*, 1661–1665.
- (266) Brooks, S. C. *Waste Characteristics of the Former S-3 Ponds and Outline of Uranium Chemistry Relevant to NABIR Field Research Center Studies*; Oak Ridge National Laboratory: Oak Ridge, TN, 2001; p 21; ORNL/TM-2001/27.
- (267) U.S. DOE. *Report on the remedial investigation of Bear Creek Valley at the Oak Ridge Y-12 Plant, Oak Ridge, TN*; Oak Ridge National Laboratory: Oak Ridge, TN, 1996; Vol. 1, p 475; DOE/OR/01-1455/v1&d1.
- (268) U.S. DOE. *Report On The Remedial Investigation of Bear Creek Valley at the Oak Ridge Y-12 Plant, Oak Ridge, TN. Appendix E. Valley-Wide Fate And Transport Report*; Oak Ridge National Laboratory: Oak Ridge, TN, 1996; Vol. 4, p 291; DOE/OR/01-1455/v4&d1.
- (269) Watson, D. B.; Moline, G. R.; Jardine, P. M.; Holladay, S. K.; Mehlhorn, T. L.; Gu, B.; Palumbo, A. V.; Spalding, B. P.; Brandt, C. C.; Doll, W. E. *Natural and Accelerated Bioremediation Research (NABIR) Field Research Center (FRC) Site Characterization Plan*; Oak Ridge National Laboratory: Oak Ridge, TN, 2001; p 93; 7212ORNL/TM-2000/269.
- (270) Wu, W. M.; Carley, J.; Fienen, M.; Mehlhorn, T.; Lowe, K.; Nyman, J.; Luo, J.; Gentile, M. E.; Rajan, R.; Wagner, D.; Hickey, R. F.; Gu, B. H.; Watson, D.; Cirpka, O. A.; Kitanidis, P. K.; Jardine, P. M.; Criddle, C. S. *Environ. Sci. Technol.* **2006**, *40*, 3978–3985.
- (271) Phillips, D. H.; Watson, D. B.; Roh, Y.; Mehlhorn, T. L.; Moon, J. W.; Jardine, P. M. *J. Environ. Qual.* **2006**, *35*, 1715–1730.
- (272) Kelly, S. D.; Kemner, K. M.; Carley, J.; Criddle, C.; Jardine, P. M.; Marsh, T. L.; Phillips, D.; Watson, D.; Wu, W. M. *Environ. Sci. Technol.* **2008**, *42*, 1558–1564.
- (273) U.S. DOE. Oak Ridge FRC site data, http://public.ornl.gov/orific/orfric6_data.cfm.
- (274) Gu, B. H.; Brooks, S. C.; Roh, Y.; Jardine, P. M. *Geochim. Cosmochim. Acta* **2003**, *67*, 2749–2761.
- (275) Zhang, F.; Luo, W. S.; Parker, J. C.; Brook, S. C.; Watson, D. B.; Jardine, P. M.; Gu, B. H. *J. Hazard. Mater.* **2011**, *190*, 863–868.
- (276) Kukkadapu, R. K.; Zachara, J. M.; Fredrickson, J. K.; McKinley, J. P.; Kennedy, D. W.; Smith, S. C.; Dong, H. L. *Geochim. Cosmochim. Acta* **2006**, *70*, 3662–3676.
- (277) Kelly, S. D.; Kemner, K. M.; Carley, J.; Criddle, C.; Jardine, P. M.; Marsh, T. L.; Phillips, D.; Watson, D.; Wu, W. M. *Environ. Sci. Technol.* **2008**, *42*, 1558–1564.
- (278) Phillips, D. H.; Watson, D. B.; Kelly, S. D.; Ravel, B.; Kemner, K. M. *Environ. Sci. Technol.* **2008**, *42*, 7104–7110.
- (279) Barnett, M. O.; Jardine, P. M.; Brooks, S. C.; Selim, H. M. *Soil Sci. Soc. Am. J.* **2000**, *64*, 908–917.
- (280) Jardine, P. M.; Sanford, W. E.; Gwo, J. P.; Reedy, O. C.; Hicks, D. S.; Riggs, J. S.; Bailey, W. B. *Water Resour. Res.* **1999**, *35*, 2015–2030.
- (281) Gu, B.; Watson, D. B.; Phillips, D. H.; Liang, L. Biogeochemical, mineralogical, and hydrological characteristics of an iron reactive barrier used for treatment of uranium and nitrate. In *Groundwater Remediation of Trace Radionuclides, and Nutrients with Permeable Reactive Barriers*; Naftz, D. L., Morrison, S. J., Davis, J. A., Fuller, C. C., Eds.; Academic Press: New York, 2002; pp 305–342.
- (282) Jardine, P. M. Influence of coupled processes on contaminant fate and transport in subsurface environments. In *Advances in Agronomy*; Sparks, D. L., Ed.; Academic Press: New York, 2008; Vol. 99, pp 1–99.
- (283) Wu, W. M.; Carley, J.; Fienen, M.; Mehlhorn, T.; Lowe, K.; Nyman, J.; Luo, J.; Gentile, M. E.; Rajan, R.; Wagner, D.; Hickey, R. F.; Gu, B. H.; Watson, D.; Cirpka, O. A.; Kitanidis, P. K.; Jardine, P. M.; Criddle, C. S. *Environ. Sci. Technol.* **2006**, *40*, 3986–3995.
- (284) Wu, W. M.; Carley, J.; Luo, J.; Ginder-Vogel, M. A.; Cardenas, E.; Leigh, M. B.; Hwang, C. C.; Kelly, S. D.; Ruan, C. M.; Wu, L. Y.;

Van Nostrand, J.; Gentry, T.; Lowe, K.; Mehlhorn, T.; Carroll, S.; Luo, W. S.; Fields, M. W.; Gu, B. H.; Watson, D.; Kemner, K. M.; Marsh, T.; Tiedje, J.; Zhou, J. Z.; Fendorf, S.; Kitanidis, P. K.; Jardine, P. M.; Criddle, C. S. *Environ. Sci. Technol.* **2007**, *41*, 5716–5723.

(285) Hunter, D. B.; Bertsch, P. M. *J. Radioanal. Nucl. Chem.* **1998**, *234*, 237–242.

(286) Morris, D. E.; Allen, P. G.; Berg, J. M.; Chisholm-Brause, C. J.; Conradson, S. D.; Donohoe, R. J.; Hess, N. J.; Musgrave, J. A.; Tait, C. D. *Environ. Sci. Technol.* **1996**, *30*, 2322–2331.

(287) U.S. Geological Survey. Abandoned mine lands initiative—providing science for watershed issues. In *Abstracts of the 11th Annual U.S. Geological Survey, Central Region, 1999 Poster Review. U.S. Geological Survey Open-File Report 99-321*; Modreski, P. J., Ed.; U.S. Geological Survey: Denver, CO, 1999; pp 29–30.

(288) Naftz, D. L.; Fuller, C. C.; Davis, J. A.; Morrison, S. J.; Feltcorn, E. M.; Freethey, G. W.; Rowland, R. C.; Wilkowske, C.; Piana, M. J. Field demonstration of three permeable reactive barriers to control uranium contamination in groundwater, Fry Canyon, Utah. In *Handbook of Groundwater Remediation Using Permeable Reactive Barriers. Application to Radionuclides, Trace Metals, and Nutrients*; Naftz, D. L., Morrison, S. J., Davis, J. A., Fuller, C. C., Eds.; Academic Press: San Diego, CA, 2002; pp 401–434.

(289) Naftz, D. L.; Feltcorn, E. M.; Fuller, C. C.; Wilhelm, R. G.; Davis, J. A.; Morrison, S. J.; Freethey, G. W.; Piana, M. J.; Rowland, R. C.; Blue, J. E. *Field Demonstration of Permeable Reactive Barriers to Remove Dissolved Uranium from Groundwater, Fry Canyon, Utah, September 1997 through September 1998 Interim Report*; U.S. Environmental Protection Agency: Washington, DC, 2000; p 89.

(290) EPA. *Cost and Performance Report. In Situ Permeable Reactive Barriers for Contaminated Groundwater at Fry Canyon, Southeastern Utah*; U.S. Environmental Protection Agency, Office of Solid Waste and Emergency Response Technology Innovation Office: Washington, DC, 2000; p 13.

(291) Morrison, S. J.; Naftz, D. L.; Davis, J. A.; Fuller, C. C. Introduction to groundwater remediation of metals, radionuclides, and nutrients with permeable reactive barriers. In *Handbook of Groundwater Remediation using Permeable Reactive Barriers. Application to Radionuclides, Trace Metals, and Nutrients*; Naftz, D. L., Fuller, C. C., Davis, J. A., Morrison, S. J., Feltcorn, E. M., Freethey, G. W., Rowland, R. C., Wilkowske, C., Piana, M. J., Eds.; Academic Press: San Diego, CA, 2002; pp 1–15.

(292) Fuller, C. C.; Piana, M. J.; Bargar, J. R.; Davis, J. A.; Kohler, M. Evaluation of apatite materials for use in permeable reactive barriers for the remediation of uranium-contaminated groundwater. In *Handbook of Groundwater Remediation Using Permeable Reactive Barriers. Application to Radionuclides, Trace Metals, and Nutrients*; Naftz, D. L., Morrison, S. J., Davis, J. A., Fuller, C. C., Eds.; Academic Press: San Diego, CA, 2002; pp 255–280.

(293) Fuller, C. C.; Bargar, J. R.; Davis, J. A. *Environ. Sci. Technol.* **2003**, *37*, 4642–4649.

(294) Fuller, C. C.; Bargar, J. R.; Davis, J. A.; Piana, M. J. *Environ. Sci. Technol.* **2002**, *36*, 158–165.

(295) LoPresti, V.; Conradson, S. D.; Clark, D. L. *J. Alloys Compd.* **2007**, *444*, 540–543.

(296) Neu, M. P.; Runde, W. H.; Clark, D. L.; Conradson, S. D.; Efurud, D. W.; Janecky, D. R.; Kaszuba, J. P.; Tait, C. D.; Haire, R. G. *Abstr. Pap. Am. Chem. Soc.* **1999**, *218*, U1084–U1084.

(297) Clark, D. L.; Choppin, G. R.; Dayton, C. S.; Janecky, D. R.; Lane, L. J.; Paton, I. *J. Alloys Compd.* **2007**, *444*, 11–18.

(298) Clark, D. L.; Janecky, D. R.; Lane, L. J. *Phys. Today* **2006**, *59*, 34–40.

(299) Santschi, P. H.; Roberts, K. A.; Guo, L. *Environ. Sci. Technol.* **2002**, *36*, 3711–3719.

(300) Xu, C.; et al. *Environ. Sci. Technol.* **2008**, *42*, 8211–8217.

(301) Brown, G. E., Jr.; Calas, G.; Hemley, R. J. *Elements* **2006**, *2*, 23–30.